# ANALYSIS OF SHEAR TEST STRUCTURE

R. O. Ford
M. D. Vanderbilt



Structural Research Report No. 4
Civil Engineering Department
Colorado State University
Fort Collins, Colorado 80521

June, 1970

CER69-70MDV-ROF43

TABLE OF CONTENTS





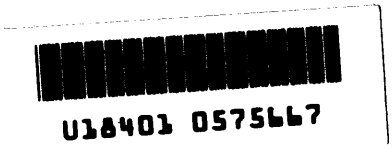

# LIST OF TABLES

## LIST OF FIGURES

LIST OF FIGURES (Continued)

Figure No. Page

# CHAPTER 1

# INTRODUCTION

## 1.1 Object

Because of the possibility of shear failure in flat plate concrete floor systems, many investigators have performed shear tests to obtain some relationship between shear strength and the concrete and slab characteristics. Previous test programs were performed using specimens assumed to represent the region of a flat plate around the column which was located inside the lines of contraflexure for principle moments. However, these test specimens did not correctly model real structures in terms of deflections, shears, in-plane forces and shape of lines of contraflexure. Therefore, the object of this test program was to test models of a reinforced concrete test specimen which simulate the behavior of a continuous multi-panel flat plate structure around an interior column.

## 1.2 Scope

This report is based on the construction and tests to failure of 15 reinforced concrete, flat plate structures made with normal-weight aggregate. Analysis of the shear strength of the specimens

is given in this report and the behavior of the specimens is given in a report by Shilling (17)*.

The test specimens were 10' - 6" square with a two inch thick slab and spandrel beams nine inches deep by six inches wide. A square or round column stub was cast in the center of each specimen. The test variables were the ratio of column size to effective depth (r/d), the ratio of reinforcement and the column shape.

A complete description of the mounting, instrumentation and testing procedure is given in Chapter 2. An analysis of the test structure is given in Chapter 3 by comparing the test failure loads to ultimate loads predicted by previously developed empirical and semi-theoretical formulas. A summary of the report, discussion and conclusions are given in Chapter 4. Appendix A contains a detailed description of the reaction dynamometers and Appendix B contains a detailed description of the shear crack detectors.

## 1.3 Acknowledgments

This report was written as a Master's Thesis under the guidance of Dr. M. D. Vanderbilt, Associate Professor of Civil Engineering. A National Defense Education Association Fellowship and a grant from the National Science Foundation made this study possible.

*Numbers in parantheses refer to entries in the bibliography.

Cement for the project was provided by the Ideal Cement Company at LaPorte, Colorado. The test was carried out at the Structural Engineering Laboratory at the Colorado State University Engineering Research Center.

## 1.4 Notation

Below are the definitions of symbols used throughout the report.

B = diameter of circular columns or for square columns the diameter of a circular column of equal area.

b = critical shear perimeter taken at the column.

C = diameter of area inside inflection lines

d = effective depth from compressive face of concrete to centroid of tensile steel.

$f'_c$ = compressive cylinder strength of concrete.

$f_{sp}$ = splitting strength of concrete.

$f_y$ = yield strength of steel.

p = reinforcing ratio.

$q = pf_y/f'_c$ = reinforcing index.

r = length of side of square column or b/4 for round columns.

$V_u$ = ultimate shear load.

$v_u = V_u/bd$ = shear stress at critical section.

Vcalc = calculated shear strength.

Vflex = shear at ultimate calculated flexural capacity of specimen.

Vtest = failure load of test specimen.

$\phi$ = Vtest/Vflex.

# CHAPTER 2

# CONDUCT OF TESTING

## 2.1 Introductory Remarks

Extensive preparations had to be made before the specimens could be tested. Section 2.2 gives a description of the test specimens used in this test series. A complete listing of all of the variables is given in Table 2.1. The procedure used in mounting the test specimens in the test frame is presented in Section 2.3. Instrumentation that was employed to obtain all the data is described in Section 2.4. Finally, the procedure used in testing the specimens to failure is given in Section 2.5.

## 2.2 Description of the Test Specimens

The shear test specimens used in these experiments were 10' - 6" square with the actual slab being 9' - 6" square as shown in Figure 2.1. The slab was two inches thick with an effective depth of 1.5 inches measured to the contact surface between the two layers of positive or negative steel. The column stub was cast monolithically with the slab at the test specimen centers. The r/d ratios of these slabs varied from two to eight. The two reinforcing ratios tested were 1% and 2% for negative reinforcement over the column stub. All slabs contained positive steel ratios

which were one-half the negative steel ratios of the center reinforcing mat. The ratio of negative slab steel around the slab perimeter was 1% for all specimens. The dimensions and locations of the steel are shown in Fig. 2.2 and 2.3. The reinforcement in the slab portion of the specimens consisted of No. 2 deformed bars while the spandrel beams had reinforcement consisting of No. 6 bars with No. 3 stirrups. All mats were rigidly tied before being placed in the form. The slabs were cast and allowed to cure five days or longer before being removed from the form.

One of the first trial slabs had a stub on top of the slab with side dimensions equal to the column dimensions. Because of difficulties in testing this slab, the top stub was deleted for the remaining specimens.

Table 2.1 contains a complete list of all the parameters and test failure loads of the current test series. All the slabs that were tested to failure were given mark numbers shown in the table. The first number in the mark is the r/d ratio, the letter stands for the shape of the column either square (S) or circular (C), the third digit gives the steel reinforcement ratio in percent for the negative steel over the column and the last digit(s) shows the sequence. Some of the slabs with circular columns did not have integer r/d ratios so the mark shows the nearest integer for r/d. The compressive strength and splitting strength of the concrete of each

slab are given in Table 2. 1. Splitting tests were not performed for the first three slabs. Therefore, in order to obtain $f_{sp}$ values for these specimens, a relationship between splitting strength and cylinder strength was determined using the other test data with the result, $f_{sp} = 6.1\sqrt{f'_c}$. Values in the last two columns were found using the relations $V_u/bd$ and $V_u/bd\sqrt{f'_c}$, respectively.

## 2. 3 Mounting of Each Specimen

Each test specimen was cast in a form at some distance away from the test stand. In order to facilitate movement of each slab to the test frame, 3/8 inch diameter bolts were cast in place in the four corners of the specimen. After the slab had cured, a strain gage was mounted on the top of the slab two inches from the column to evaluate stresses during moving.

A fork lift was used to lift the slab from the form and to carry it to the test frame located in the north end of the lab. The strain gage was connected to a strain indicator and the resulting strain due to the lifting of the slab was recorded. The average strain for all test specimens was about 60 micro-inches per inch with the peak for one slab reaching $120 \times 10^{-6}$. If Young's Modulus for concrete is assumed as 3,000,000 psi then the peak stress during moving was 360 psi. It may be concluded that no cracking of the concrete occurred during moving.

The test frame contained five concrete columns with reaction dynamometers mounted on the tops. Steel reaction beams and columns completed the framework as shown in Fig. 2.4 and 2.5.

The slab was carried to the test frame and lowered to the four corner dynamometers. The center dynamometer was mounted on a set of 1-3/4 inch diameter bolts so that vertical movement was possible. To remove the strain in the slab that was incurred through transport, the center load cell was raised until the strain reading in the slab gage returned to zero and then the dynamometer was secured. It was assumed that stresses in the slab portion around the column were then close to the initial state of stress that existed in the form.

## 2.4 Instrumentation

A vinyl air pressure bag was used as the loading device for applying a uniform load over the surface of the slab as shown in Fig. 2.6 and 2.7.* The pressure was monitored by a pressure gage with a double check made with a mercury or water manometer.

Force reactions were measured by the use of the dynamometers located at the four corners and at the central column. A complete description of these reaction cells is given in Appendix A. The reaction cells and the slab gage were all connected to a strain

*The air bag was manufactured by Richardardson Manufacturing Co., a Fort Collins firm which specializes in the manufacture of gymnasium wrestling mats.

indicator through two Budd ten channel switch and balance units as shown in Fig. 2.8.

Two crack detectors were used to monitor the formation of the shear crack in the slab. These crack detectors are described in Appendix B. The strains that the crack detectors produced were read through a Hathaway 20 channel strain indicator; see Fig. 2.8.

Electrical resistance strain gages were also mounted on the columns for several slabs starting with slab 6C1-9. The strain gages were University Precision Type 60 with a gage factor of 2.05, a length of .6 inches and a resistance of 120 ohms. These were located along one side of square columns and one quadrant on round columns as shown in Fig. 2.9 and 2.10.

Deflection dials were mounted under the slabs. They were located on center lines from the central column to the spandrel beam on the west side and in the southwest corner. The accuracy of most gages was 0.001 inch. See Fig. 2.9 and 2.10 for locations.

## 2.5 Testing Sequence

Each slab required extensive preparation before the testing could be performed. Length measurements were taken to make certain that dimensions of the slab did not vary significantly from the 9' - 6" desired. The column gages, where used, were then applied with epoxy and later were wired. Next, the slab gage was wired and the crack detectors mounted.

The slightly oversized vinyl air bag was placed on the slab. Sections of plywood were placed at the edges and center of the bag and then two reaction panels were put in place. The plywood sections were used to seal any gaps between the panels and spandrel beams. The bag and panels were situated inside the upper portion of the spandrel beams as shown in Fig. 2.6. Essentially the confined bag acted as an "innertube" and was able to sustain test pressures of over 5 psi while in an unconfined condition the bag split at the seam at a pressure of less than 2 psi. Finally, the steel reaction beams were put in place over the reaction panels. Fig. 2.12 shows the completed test setup.

All data recording devices were then zeroed. To do this correctly, the plywood reaction panels were lifted from the slab and strapped to the reaction beams. This gave a zero load on the test specimen.

Static loads were applied to the specimens. The air pressure, vertical reaction at the center dynamometer and one crack detector were monitored throughout the loading. Loads were applied in steps and complete sets of data readings were taken every one-half psi. Load increments near the predicted failure load were reduced so the slab reactions could be studied more carefully. The specimen was loaded to failure with a reading being made of the vertical reaction of the center dynamometer at failure.

At one, two and three psi and at failure, the flexural cracks that formed on the bottom of the slab were marked. An illuminated seven-power lens was used to thoroughly examine the bottom surface.

All of the loading equipment was then removed so that the final set of data could be obtained. Photographs were taken of the wedge section that punched through the slab, with and without the shattered concrete in place. Measurements were made of the shear crack so that a slope could be determined. The slab was then lifted from the frame, the bottom surface was photographed and the specimen was thereupon discarded.

# CHAPTER 3

# ANALYSIS

## 3.1 Introductory Remarks

Many shear strength equations have been developed in past years. The more recent equations and methods of analysis are presented in section 3.2(a). The current test series is analysed using the equations presented in section 3.2(a) with a summary of the results being given in section 3.2(b). The calculated values of shear strength are given in Tables 3.1 and 3.2 with a comparison being made between Vcalc, the calculated shear strength, and Vtest, the tested shear strength.

## 3.2 Comparison of Measured and Computed Strengths Using Existing Formulas

### (a) Review of Existing Formulas

The equation developed by Moe (15) is probably the most studied shear strength equation, having been used by many experimentalists since its development. Moe tested forty-three specimens that were 72 inches square by 6 inches deep. He varied the column size, steel orientation and size and position of holes near the column. His specimens were assumed to represent the

region of negative bending around a column in a medium-sized flat plate floor slab. The assumed span length of the prototype would be 15 feet. The equation Moe devised is good only for the range of r/d between 0.9 and 3.1.

The equation developed by Moe is

$$\frac{v_u}{\sqrt{f'_c}} = \frac{V_u}{bd\sqrt{f'_c}} = \frac{15(1 - 0.075\ r/d)}{1 + 5.25\ bd\sqrt{f'_c}/Vflex} \quad . - - - (3.1)$$

The term Vflex is included in this equation as a result of a theory of shear failure developed earlier by Hognestad (7) which related shear strength to Vflex. The term $\sqrt{f'_c}$ was used because shear failure was of a splitting type somewhat like specimens under tension. The ratio r/d has an effect on shear strength since shear stress has been observed to increase with decrease in r/d ratios. Through a statistical analysis, Moe obtained the constants in his equation.

Moe developed two design equations taking into consideration values of r/d which were less than 3 and greater than 3. These equations are:

$$v = (9.23 - 1.12\ r/d)\sqrt{f'_c} \quad r/d < 3 \quad , - - - (3.2)$$

$$v = (2.5 + 10\ r/d)\sqrt{f'_c} \quad r/d > 3 \quad . - - - (3.3)$$

Hognestad, Elstner and Hanson tested six slabs corresponding to some of the slabs of Moe's test series (8). In this series of

tests, the experimenters used light-weight concrete. A plot was made of the test results comparing $V_{test}/bd\sqrt{f'_c}$ and $\phi = V_{test}/V_{flex}$. Moe's test results were included on the same graph, and Moe's equation was drawn on the graph to compare it to the test data. The equation plotted through Moe's test data but the data found by Hognestad, Elstner and Hanson plotted 25% lower. This led the experimenters to introduce splitting strength into the Moe equation in place of compressive strength. The relationship they obtained between splitting strength and compressive strength was $f_{sp} = 6.7\sqrt{f'_c}$. Substituting this into Moe's equation gave

$$v_u = \frac{V_u}{bd} = \frac{2.24\,(1 - 0.075\,r/d)\,f_{sp}}{1 + (0.784\,bd\,f_{sp}/V_{flex})} \qquad \text{- - - - (3.4)}$$

A comparison of this equation with their test data gave a better comparison.

Mowrer (16) did further tests of light weight concrete slabs. The twenty-six specimens were four feet square and three inches thick. The column size, steel reinforcement and edge conditions were the variables. The edge conditions tested were simply supported edges and clamped edges.

The twenty-six slabs were tested and analysed along with twenty-five slabs tested by Janney (10). These slabs were smaller in size than previous tests. An in-depth analysis was made using previously determined equations. The results of the analysis showed that the following equation better fit the test data.

$$\frac{V_u}{bd\sqrt{f'_c}} = \frac{9.7\,(1.0 + d/r)}{1 + 5.25\,bd\sqrt{f'_c}/Vflex} \qquad \text{- - - (3.5)}$$

This is a reanalysis of the constants in Moe's equation.

Yitzhaki made an analysis of slabs based on flexural strength (20). The equation developed was

$$V_u = 8(1 - q/2)d^2\,(144.3 + 0.164\,pf_y)(1.0 + 0.5\,r/d)\,, \quad \text{- - (3.6)}$$

which was obtained from consideration of ACI's ultimate strength theory for flexure. This equation takes into account the strength of the steel through the $pf_y$ term. The effect of concrete strength is accounted for by $(1 - q/2)$. The final variable of effective depth, r/d, completes the equation format. At a distance d from the column edge, Yitzhaki finds the nominal shear stress to be defined as

$$v_u = \frac{V_u}{(1 - q/2)(d)(4r + 8d)} = 149.3 + 0,164\,pf_y \qquad \text{, - - - (3.7)}$$

which is a function of reinforcing strength only. Previous test data were used to obtain the equation constants.

Kinnunen and Nylander experimented with sixty-one round slabs and developed a highly complicated scheme for the analysis of slabs (12). Their specimens were 171 cm (5.83 ft) in diameter, 15 cm (5.9 in) thick and columns were 5 cm, 15 cm and 30 cm in diameter. The column size and the reinforcement were the

variables with the reinforcement being in ring, radial or two-way configurations.

To obtain a solution using their equations requires the solution of many equations in an iterative technique. The variable iterated upon is the distance y from the compressive surface to an imaginary conical shell which was derived from their theoretical structure. With a chosen value of y and the slab characteristics ($f'_c$, $f_y$, p, B, C, d), the equations can be used to calculate two values of ultimate load. One value of ultimate load is found by considering the strength of the concrete and the other by considering the steel strength. If during an iteration, the two values of ultimate load are not equal, the value of y is changed until the two ultimate load values become equal. The details of the procedure are described elsewhere (3, 16).

Kinnunen restudied the results of the two-way reinforced slabs that were tested by Kinnunen and Nylander since their initial theory did not give satisfactory results for two-way reinforced slabs (13). Kinnunen added to the previous theory the effects of membrane and dowel action of the reinforcement. He concluded that these effects combined result in 35% of the total ultimate load with the dowel effect being 25%.

The technique for solving the equations developed by Kinnunen is similar to the iterative technique developed by Kinnunen

and Nylander. The series of equations to be solved is about twice the number as the Kinnunen-Nylander method. The same general theoretical structure was used in the analysis.

ACI Committee 326 studied many of the equations that had been developed prior to 1962 (2). They found that Moe's equation was the most applicable to design so the committee decided to modify that equation for use by designers.

To make the equation simpler, Committee 326 analysed the equation and rearranged its form. Since it is desirable to have the shear strength of a slab greater than or equal to the flexural strength, the committee put the ratio $\phi$ = Vtest/Vflex equal to 1.0. The resulting equation was invalid over the full range of variables used in practical design. A new equation was then developed which was

$$v_u = 4(d/r + 1)\sqrt{f'_c} \quad , - - - (3.8)$$

which is applicable at the periphery of the loaded area.

The committee felt that the basic concepts of the 1956 ACI Code should be followed in the succeeding code (1963) and suggested that the shear strength be calculated by the following equations:

$$V_u = v_u bd \ , \ v_u = 4.0\sqrt{f'_c} \quad , - - - (3.9)$$

where b is the psuedocritical section at d/2 from the loaded area.

The limit on $v_u$ was obtained by letting r/d approach infinity in equation 3.8. This latter set of equations was accepted by the ACI Committee 318 for the 1963 Building Code Requirements for Reinforced Concrete.

(b) Comparison of Strengths

Fig. 3.1 shows a plot of the test data in terms of $V_u/bd\sqrt{f'_c}$ against the r/d ratios. The circle or square depicts the shape of column and the post script is the percent negative steel existing over the column. Comparing the points for each separate r/d ratio shows that the slabs with circular columns had larger ultimate shearing strengths than did the square columns of equal steel percentage. Stress concentrations in the square columns, as explained later, appear to be the reason for this phenomenon. Also, Fig. 3.1 shows that the slabs with higher steel ratios failed at higher stresses for constant r/d ratios. The change in steel percentage did not affect the strengths of slabs having the larger columns as much as it did for the smaller columns. Dowel and membrane actions could explain part of the higher stresses for the 2% steel slabs.

Tables 3.1 and 3.2 show the analysis of the test series using the formulas and methods described in section 3.2(a). The shear loads at ultimate flexural strength of the slabs were computed by Shilling (17). Columns headed with VHHE, V158 and V198 in Tables 3.1 and 3.2 are results of equations by Hognestad, Hanson

and Elstner, Kinnunen and Nylander and Kinnunen, respectively. VMOE was computed using equation 3.1 and VYITZ was computed using equation 3.6. Following the columns of computed strengths are columns giving the ratio of computed strength to failure strength (Vcalc/Vtest) with the mean, median and standard deviation given at the bottom of the columns. The upper and lower limits of Vcalc/Vtest found by each of the equations are underlined in the tables.

Of the previously developed equations, Moe's gives the best mean-standard deviation combination of 1.003 for the mean and .204 for the standard deviation. Kinnunen's method gives a surprisingly good mean of 1.01 considering the magnitude of difficulty that exists in applying this extremely complex method. However, the predicted strengths showed a large scatter giving a standard deviation at .300. The other equations show poorer predictions of failure strengths. The conservatism of the ACI Code equation is shown by the low mean of .618.

All of the computations shown in Tables 3.1 and 3.2 were obtained with the use of the Colorado State University Control Data Corporation 6400 electronic computer. The Kinnunen-Nylander and Kinnunen methods proved quite difficult to program.

The average Vcalc/Vtest values for specific r/d ratios are shown graphically in Fig. 3.2. Using this plot and Tables 3.1 and

3.2, it can be seen that no one particular equation appears better than the others over the full r/d range.

# CHAPTER 4

# SUMMARY, DISCUSSION AND CONCLUSIONS

## 4.1 Summary

This report describes tests on 15 specimens of a new shear test structure. The specimens were 10' - 6" square with a two inch slab. Spandrel beams were nine by six inches making the actual slab 9' - 6" square as shown in Fig. 2.1. A square or circular column stub was cast monolithically with the slab in the center of the specimen. The variables were the r/d ratio, reinforcement ratio and column shape.

The slabs were tested on a five column test frame with a uniform static load being applied with a vinyl air bag as shown in Fig. 2.6. Reactions at the five columns, deflections, load at initial shear cracking and strains near the slab of some of the columns constituted the data taken. The test sequence consisted of loading the specimens to failure while making data readings at every one-half psi or smaller increment. Details of the test sequence are given in Chapter 2.

An analysis of the ultimate load for the current test series was made using the newer of the previously developed shear strength equations. A comparison between Vcalc and Vtest was

made to show which equation best predicted strengths. The equation developed by Moe gave the best results. However, none of the equations were reliable throughout the range of r/d studied. Details of the analysis are given in Chapter 3.

Appendix A gives a description of the reaction dynamometers used in the test program. Appendix B gives a description of the shear crack detectors.

## 4.2 Discussion

Fig. 4.1 and 4.2 show reactions for slabs 8S1-6 and 8C1-13 for various loads. All vertical reactions at the four corners varied by not more than 22% in relation to each other. It was generally the case that the reactions at A and C were larger than those and B and D. Because the magnitude of the reactions at the four corners were not equal, there could possibly have been some anti-symmetry in the loading or test specimens. The distribution of the reactions between columns for all slabs had the same general pattern as shown in Fig. 4.1 and 4.2.

The reaction at the center column varied between 27% and 43% of the total reaction throughout the range of loading as can be seen in Fig. 4.3. The tests plotted in Fig. 4.3 are the slabs which produced the upper and lower ratios of percent of column reaction to total reaction along with one of the slabs that gave intermediate values. All other slabs plot somewhere in between the limits

shown. The average of column reaction to total reaction is about 35% at failure. An elastic study of the specimens made by Janowski (11) showed the columns should carry about 50% of the total load.

Strains in the columns of slabs 6C1-9, 2C1-11 and 6S2-14 are shown in Fig. 4.4, 4.5 and 4.6, respectively. Fig. 4.5 shows results for only three gages because gages one and two failed to work during the test. For the square column, 6S2-14, the strains verify the findings of other researchers that a stress concentration is present at the corners (9, 11, 15). For circular columns, the strains show that the stress is fairly uniform around the column periphery. The difference in stresses between the two columns helps explain why the circular columns failed at higher stresses than square columns of equal perimeter.

The crack detectors showed that the shear cracks opened at loads greater than 50% of the ultimate load. The crack detectors that were on the corner of the column showed shear crack opening before those on the side of the column on most slabs. Larger principle moments and stress concentrations in the corner of the columns caused the shear crack to open there first.

The current test series comes closer to representing real structures than most of the previous test programs. Analysis of the data obtained with the previously developed equations seems to

show that there are several factors that should be contained within an equation which will accurately predict shear strengths. As can be seen by Fig. 3.2, four of the strength equations (Hognestad, Hanson and Elstner, Moe, Yitzhaki, and Kinnunen) give fairly decent plots of the average Vcalc/Vtest for specific r/d ratios. A look at the mean and standard deviations of Vcalc/Vtest for these equations shows that the equations have a large spread in the predictions of shear strengths.

Moe's, Hognestad, Hanson and Elstner's and Yitzhaki's equations are all dependent upon the flexural strength of the slabs. Yitzhaki based the flexural strength of his equation on the moment capacity of the slab while Moe and Hognestad, et al, based flexural strength on a yield line analysis of the slab. Obtaining the Vflex terms for Moe's and Hognestad's equations through yield line analyses prove quite difficult for most continuous structures. A sophisticated yield analysis will usually give a value for Vflex that will allow Moe's and Hognestad's equations to predict the ultimate loads fairly accurately. However, VMOE and VHHE are very sensitive to Vflex. The flexural strength term used by Yitzhaki is a more easily and definitely defined quantity and thus the ultimate values found using Yitzhaki's equation are not dependent upon ill defined parameters.

Kinnunen's method considers membrane and dowel effects of the reinforcing steel on shear capacity along with properties of

the concrete and steel. The test data plotted in Fig. 3.1 shows that the dowel and membrane effects may be present in the slabs.

The other factors that appear to be important are the steel yield strength, column size and effective depth to the reinforcing steel. These parameters are readily determined for any one slab and since the previously developed equations contain these variables and give fair results using them, the parameters appear to be important in predicting the ultimate capacity of the slab.

The main problem is that there is an excessive deviation in the predicted strength using these equations. This problem could arise because the parameters are not related correctly. A re-analysis of the constants in Moe's, Hognestad's and Yitzhaki's equations using the current test data could be accomplished to form equations that would give better means and standard deviations for the current test series than do the present equations. However, this method of finding an equation is based in part on the values of the term Vflex which is in itself hard to find.

ACI Committee 326 has produced equation (3.9) that gives a small standard deviation of the Vcalc/Vtest values for the current test data. An equation similar to this with the safety factor not as great would probably be fairly accurate at predicting the ultimate shear capacities of slabs even though some of the previously mentioned parameters are not included in the equation. For example,

if the 4.0 $\sqrt{f'_c}$ in Equation (3.9) is replaced by 6.0 $\sqrt{f'_c}$ good agreement between Vtest and Vcalc is obtained for all r/d values.

## 4.3 Conclusions

Fig. 4.7 shows a plot of $V_u/bd\sqrt{f'_c}$ for the current test series along with those of previous test programs. By comparing the points plotted the conclusion can be made that the test specimens of this series produce results comparable to the other test programs. However, the data for the current series plot somewhat higher on the average than the data for the other test series. A possible reason for the current test data plotting higher is that the test specimens had the additional force and physical effects which exist in real structures.

The results from the crack detectors showed that the shear cracks usually opened at the column corners before opening in the sides. The strain gages showed that stress concentrations existed in the square columns at the corners near the joint with the slab. The analogy which best explains the stress concentrations is that of a flat plate (a sheet of paper) resting on four points (fingers of the hand) which represents the corners of a column. Loading the plate outside the four points results in the lifting of the plate portion within the points generating a concentration of reactions at the four points (corners). A square column reacts generally in the same

way. The column strain gages also showed that round columns had a nearly uniform stress distribution near the slab connection.

Because of the problems encountered in computing the shear load of a column at the flexural capacity of the slab, the theories involving the Vflex term obtained through yield line analysis should not be depended upon to give shear strengths of slabs unless a 50% error is tolerable. A new shear strength equation better relating the shear strength parameters needs to be developed although considering the scatter shown in Fig. 4.7, it appears doubtful that a universally consistent equation can be developed.

# BIBLIOGRAPHY


1. American Concrete Institute, "ACI Standard Building Code Requirements for Reinforced Concrete," The Institute, Detroit, 1963, 144 p., (ACI 318 - 63).

2. ACI-ASCE Committee 326, "Shear and Diagonal Tension," American Concrete Institute, Proceedings, 59:352 - 96, March, 1962.

3. Criswell, M. E., "Strength and Behavior of Reinforced Concrete Slab-Column Connections Subjected to Static and Dynamic Loadings," University of Illinois, Urbana, 1970, (Doctor's Thesis).

4. Elstner, R. C. and Hognestad, E., "Shearing Strength of Reinforced Concrete Slabs," American Concrete Institute, Journal, 18:29 - 58, July, 1956.

5. Guralnick, S. and LaFraugh, R., "Laboratory Study of a 45 - Foot Square Flat Plate Structure," American Concrete Institute, Journal, 60:1107 - 85, September, 1963.

7. Hognestad, E., "Shearing Strength of Reinforced Concrete Column Footings," American Concrete Institute, Journal, 25:189 - 208 (1953).

8. Hognestad, E., Elstner, R. D., and Hanson, J., "Shear Strength of Reinforced Structural Lightweight Aggregate Concrete Slabs," American Concrete Institute, Journal, 61:643 - 56, June, 1964.

9. Ivy, C. B., "The Diagonal Tension Resistance of Structural Lightweight Concrete Slabs," Texas A & M University, 1966, 100 p., (Doctor's Thesis).

10. Janney, R., "Shear Strength of Flat Plate-Column Connection in Reinforced Concrete," Colorado State University, Fort Collins, Colorado, 1965, 104 p., (Master's Thesis).

11. Janowski, R. H., "Elastic Analysis of Shear Test Plate," Colorado State University, Fort Collins, Colorado, 1970, 91 p., (Master's Thesis).

12. Kinnunen, S. and Nylander, H., "Punching of Concrete Slabs Without Shear Reinforcement," Swedish Royal Institute of Technology, Transactions, No. 158, Stockholm, 1960, 112 p.

13. Kinnunen, S., "Punching of Slabs With Two-Way Reinforcement With Special Reference to Dowel Effect and Deviation of Reinforcement from Polar Symmetry," Swedish Royal Institute of Technology, Transactions, No. 198, Stockholm, 1963, 109 p.

14. Magura, D. D., and Corley, W. G., "Test to Destruction of a Multipanel Waffle Slab Structure," National Academy of Sciences-National Research Council, Washington, D. C., 1968, 118 p.

15. Moe, J., "Shearing Strength of Reinforced Concrete Slabs and Footings Under Concentrated Loads," Portland Cement Association Research and Development Laboratories, Development Department, Bulletin D47, Skokie, Illinois, April, 1961, 135 p.

16. Mowrer, R. D., "A Study of the Shear Strength of Lightweight Reinforced Concrete Flat Plates," Colorado State University, Fort Collins, Colorado, 1963, 77 p., (Master's Thesis).

17. Shilling, R., "Behavior of Punching Shear Specimen," Colorado State University, Fort Collins, Colorado, 1970, (Master's Thesis).

18. Whitney, C. S., "Ultimate Strength of Reinforced Concrete Flat Slabs, Beams and Frame Members Without Shear Reinforcement," American Concrete Institute, Journal, 29:265 - 298 (1957).

19. Vanderbilt, M. D., Sozen, M. A., and Siess, C. P., "Deflection of Reinforced Concrete Floor Slabs," Illinois University Department of Civil Engineering, Structural Research Series No. 263, Urbana, Illinois, April, 1963, 287 p.

20. Yitzhaki, D., "Punching Strength of Reinforced Concrete Slabs," American Concrete Institute, Journal, 63:527 - 40, May, 1966.

| MARK | b | r | d | r/d | $u^-$ | $u^+$ | $f'_c$ | $f_{sp}$ | $f_y$ | $V_u$ | $v_u$ | $v_u/\sqrt{f'_c}$ |
|---|---|---|---|---|---|---|---|---|---|---|---|---|
| | in. | in. | in. | | | | | | | | | |
| 2S1 - 1 | 12 | 3 | 1.5 | 2 | .01 | .005 | 3997 | 388 | 43.9 | 9.65 | 536 | 8.49 |
| 3S1 - 2 | 18 | 4.5 | 1.5 | 3 | .01 | .005 | 3330 | 352 | 43.9 | 10.48 | 388 | 6.72 |
| 4S1 - 3 | 24 | 6 | 1.5 | 4 | .01 | .005 | 3010 | 334 | 43.0 | 11.54 | 321 | 5.85 |
| 3C1 - 4 | 18 | 4.5 | 1.5 | 3 | .01 | .005 | 3200 | 335 | 43.0 | 13.13 | 487 | 8.61 |
| 6S1 - 5 | 36 | 9 | 1.5 | 6 | .01 | .005 | 3070 | 356 | 43.0 | 17.60 | 326 | 5.89 |
| 8S1 - 6 | 48 | 12 | 1.5 | 8 | .01 | .005 | 2970 | 323 | 42.8 | 20.28 | 282 | 5.16 |
| 2S2 - 7 | 12 | 3 | 1.5 | 2 | .02 | .01 | 3370 | 338 | 46.1 | 11.13 | 619 | 10.68 |
| 4S2 - 8 | 24 | 6 | 1.5 | 4 | .02 | .01 | 3140 | 349 | 59.6 | 15.54 | 432 | 7.67 |
| 6C1 - 9 | 35.3 | 9 | 1.5 | 5.88 | .01 | .005 | 3730 | 434 | 56.8 | 21.63 | 409 | 6.68 |
| 8S2 - 10 | 48 | 12 | 1.5 | 8 | .02 | .01 | 3810 | 418 | 56.1 | 25.65 | 356 | 5.77 |
| 2C1 - 11 | 12 | 3 | 1.5 | 2 | .01 | .005 | 2894 | 295 | 56.0 | 8.77 | 487 | 9.07 |
| 4C1 - 12 | 24.25 | 6.063 | 1.5 | 4.04 | .01 | .005 | 3215 | 422 | 56.1 | 16.30 | 448 | 7.90 |
| 8C1 - 13 | 46.5 | 11.89 | 1.5 | 7.93 | .01 | .005 | 3478 | 358 | 56.0 | 22.68 | 318 | 5.40 |
| 6S2 - 14 | 36 | 9 | 1.5 | 6 | .02 | .01 | 2993 | 300 | 57.5 | 18.01 | 334 | 6.10 |
| 4C2 - 15 | 24.3 | 6.07 | 1.5 | 4.05 | .02 | .01 | 3117 | 323 | 55.0 | 21.70 | 595 | 10.65 |

TABLE 2.1. Properties and Results of Current Test Series

| MARK | Vtest kips | Vflex kips | VMOE kips | VMOE / Vtest | VHHE kips | VHHE / Vtest | VMOWRER kips | VMOWRER / Vtest | VYITZ kips | VYITZ / Vtest |
|---|---|---|---|---|---|---|---|---|---|---|
| 2S1 - 1 | 9.65 | 24.4 | 11.66 | 1.208 | 10.86 | 1.125 | 13.30 | 1.378 | 7.53 | .780 |
| 3S1 - 2 | 10.48 | 26.7 | 13.87 | 1.323* | 12.90 | 1.231 | 15.43 | 1.472 | 9.30 | .888 |
| 4S1 - 3 | 11.54 | 25.0 | 14.66 | 1.270 | 13.69 | 1.186 | 16.93 | 1.467 | 11.02 | .955 |
| 3C1 - 4 | 13.13 | 25.3 | 13.48 | 1.027 | 12.27 | .934 | 15.00 | 1.142 | 9.23 | .703 |
| 6S1 - 5 | 17.60 | 26.6 | 15.52 | .882 | 15.12 | .859 | 21.29 | 1.210 | 14.72 | .836 |
| 8S1 - 6 | 20.28 | 31.4 | 14.22 | .701* | 13.18 | .650 | 25.86 | 1.275 | 18.33 | .904 |
| 2S2 - 7 | 11.13 | 43.7 | 11.82 | 1.062 | 10.43 | .937 | 13.49 | 1.212 | 9.34 | .839 |
| 4S2 - 8 | 15.54 | 57.7 | 17.90 | 1.152 | 16.83 | 1.083 | 20.67 | 1.330 | 15.09 | .971 |
| 6C1 - 9 | 21.63 | 38.5 | 18.82 | .870 | 19.60 | .906 | 25.47 | 1.178 | 15.89 | .734 |
| 8S2 - 10 | 25.65 | 65.0 | 19.62 | .765 | 19.78 | .771 | 35.69 | 1.391 | 25.58 | .997 |
| 2C1 - 11 | 8.77 | 29.4 | 10.53 | 1.200 | 8.86 | 1.010 | 12.01 | 1.370 | 7.84 | .894 |
| 4C1 - 12 | 16.30 | 34.3 | 16.39 | 1.005 | 17.74 | 1.088 | 18.97 | 1.164 | 11.98 | .735 |
| 8C1 - 13 | 22.68 | 39.3 | 16.15 | .712 | 15.14 | .668 | 29.00 | 1.279 | 19.81 | .873 |
| 6S2 - 14 | 18.01 | 56.2 | 19.10 | 1.061 | 16.28 | .904 | 26.20 | 1.455 | 19.66 | 1.091 |
| 4C2 - 15 | 21.70 | 52.5 | 17.67 | .814 | 15.62 | .720 | 20.46 | .943 | 14.78 | .681 |
| Mean | | | | 1.003 | | .938 | | 1.284 | | .859 |
| Median | | | | 1.026 | | .934 | | 1.279 | | .873 |
| Standard Deviation | | | | .204 | | .183 | | .147 | | .118 |

*Underline values represent high and low values within column

TABLE 3.1. Comparisons of Vcalc/Vtest for Current Test Series

| MARK | Vtest kips | Vflex kips | V158 kips | V158 / Vtest | V198 kips | V198 / Vtest | VCODE kips | VCODE / Vtest |
|---|---|---|---|---|---|---|---|---|
| 2S1 - 1 | 9.65 | 24.4 | 7.00 | .725 | 8.33 | .863 | 5.80 | .601 |
| 3S1 - 2 | 10.58 | 26.7 | 8.13 | .775 | 9.49 | .905 | 7.06 | .674 |
| 4S1 - 3 | 11.54 | 25.0 | 8.83 | .765 | 10.70 | .928 | 8.39 | .727 |
| 3C1 - 4 | 13.13 | 25.3 | 7.82 | .595 | 8.87 | .675 | 7.91 | .603 |
| 6S1 - 5 | 17.60 | 26.6 | 11.04 | .627 | 13.25 | .753 | 11.87 | .674 |
| 8S1 - 6 | 20.28 | 31.4 | 13.06 | .644 | 15.70 | .774 | 15.01 | .740 |
| 2S2 - 7 | 11.13 | 43.7 | 9.42 | .846 | 13.50 | 1.213 | 5.33 | .479 |
| 4S2 - 8 | 15.54 | 57.7 | 15.84 | 1.019 | 22.65 | 1.457 | 8.57 | .552 |
| 6C1 - 9 | 21.63 | 38.5 | 13.48 | .623 | 15.58 | .720 | 13.93 | .644 |
| 8S2 - 10 | 25.65 | 65.0 | 30.96 | 1.207 | 37.48 | 1.461 | 17.00 | .663 |
| 2C1 - 11 | 8.77 | 29.4 | 7.11 | .810 | 8.89 | 1.014 | 5.88 | .670 |
| 4C1 - 12 | 16.30 | 34.3 | 11.73 | .720 | 13.61 | .835 | 8.38 | .514 |
| 8C1 - 13 | 22.68 | 39.3 | 16.52 | .728 | 19.54 | .861 | 15.70 | .692 |
| 6S2 - 14 | 18.01 | 56.2 | 22.27 | 1.237 | 29.68 | 1.648 | 11.72 | .651 |
| 4C2 - 15 | 21.70 | 52.5 | 17.15 | .791 | 22.58 | 1.040 | 8.27 | .381 |
| Mean | | | | .808 | | 1.010 | | .618 |
| Median | | | | .765 | | .905 | | .651 |
| Standard Deviation | | | | .199 | | .300 | | .099 |

TABLE 3.2. Comparisons of Vcalc/Vtest for Current Test Series

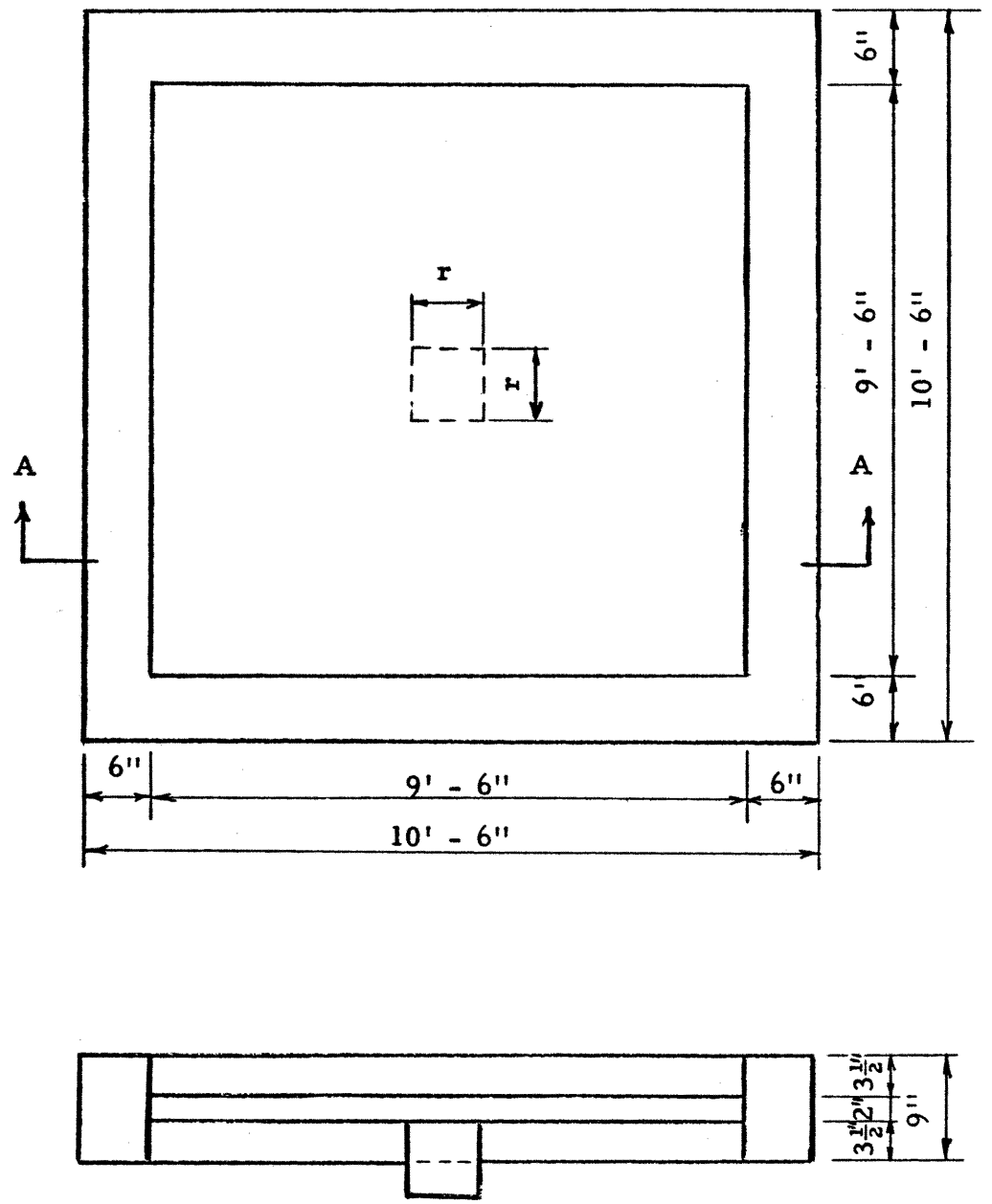


Section A - A

Fig. 2.1. Typical Test Specimen

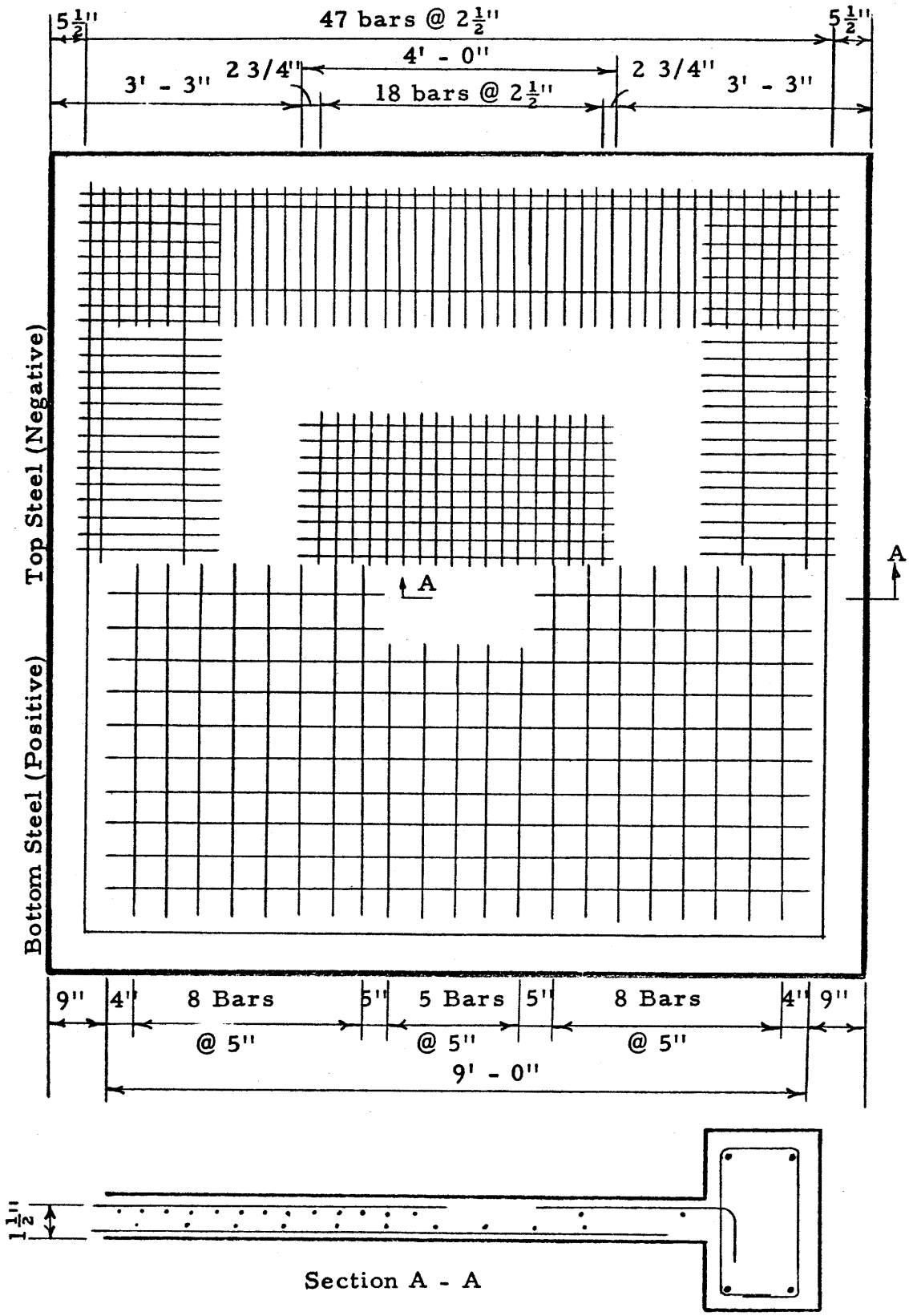


Fig. 2.2. One Percent Steel Arrangement

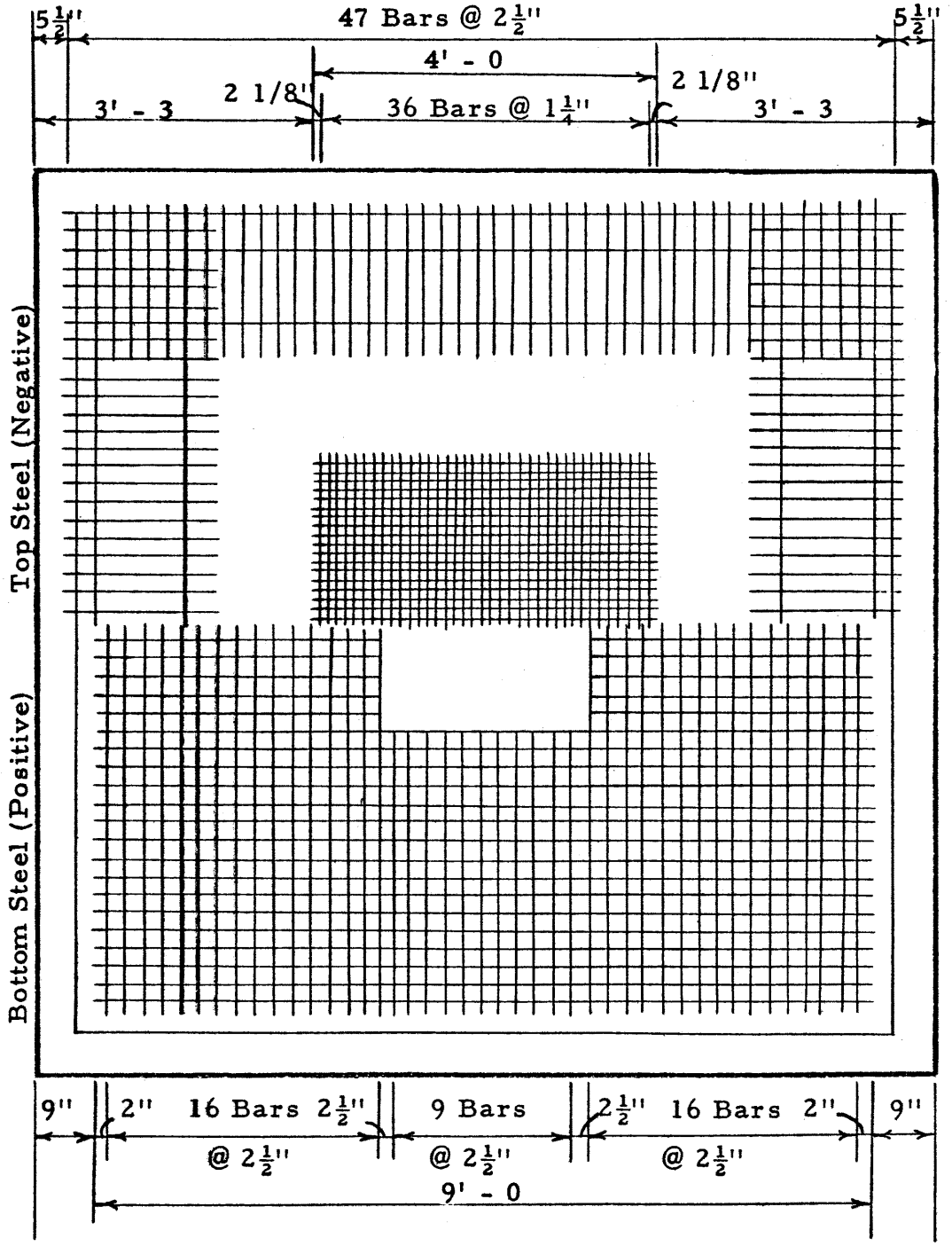


**Fig. 2.3.** Two Percent Steel Arrangement

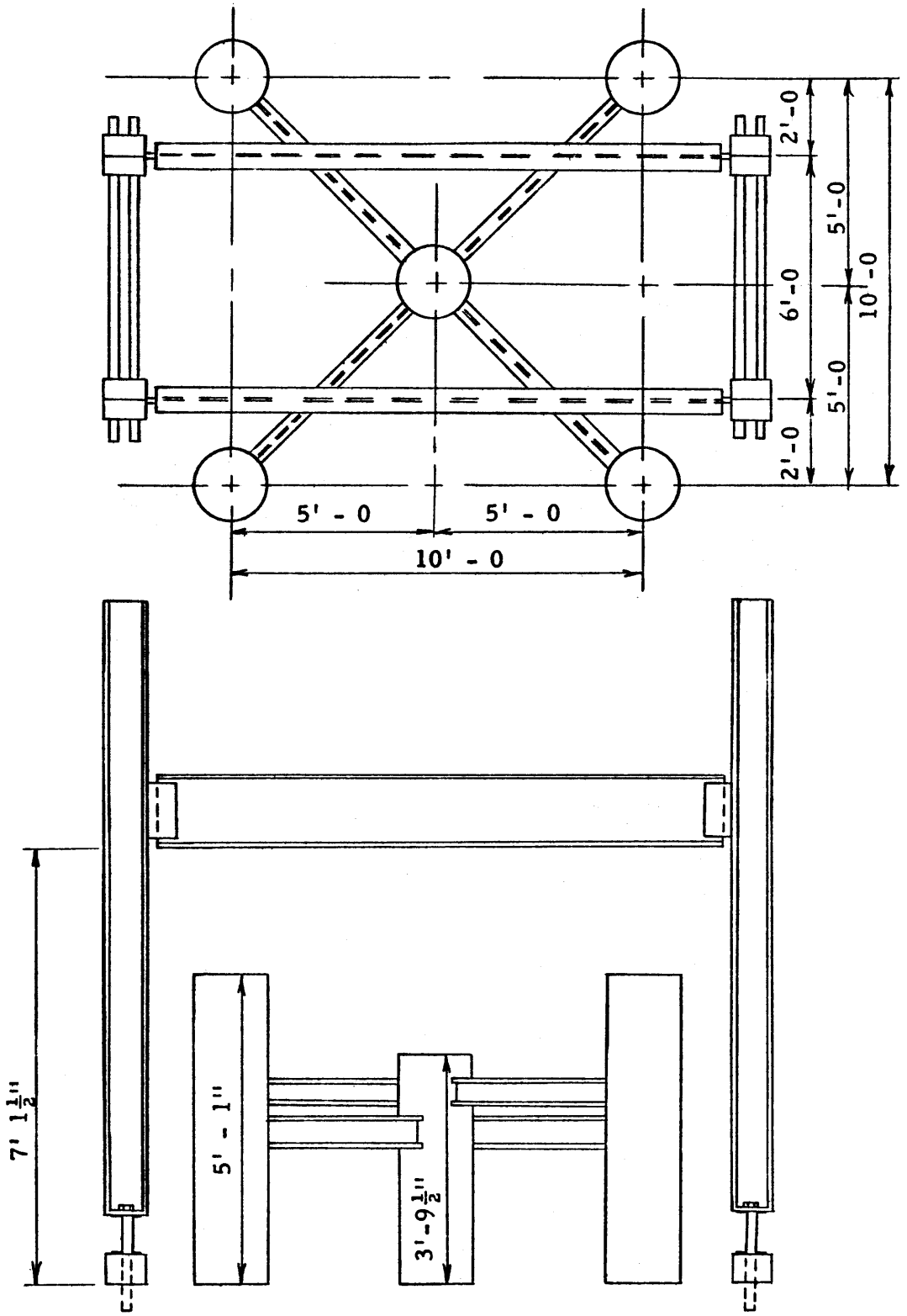


Fig. 2.4. Test Frame

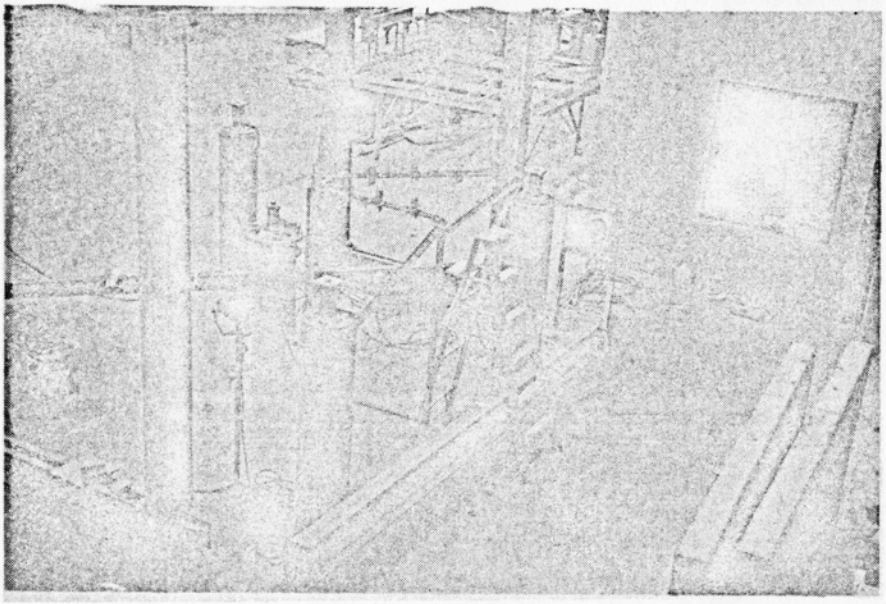

Fig. 2.5. Test Frame Photograph
With Beams Down

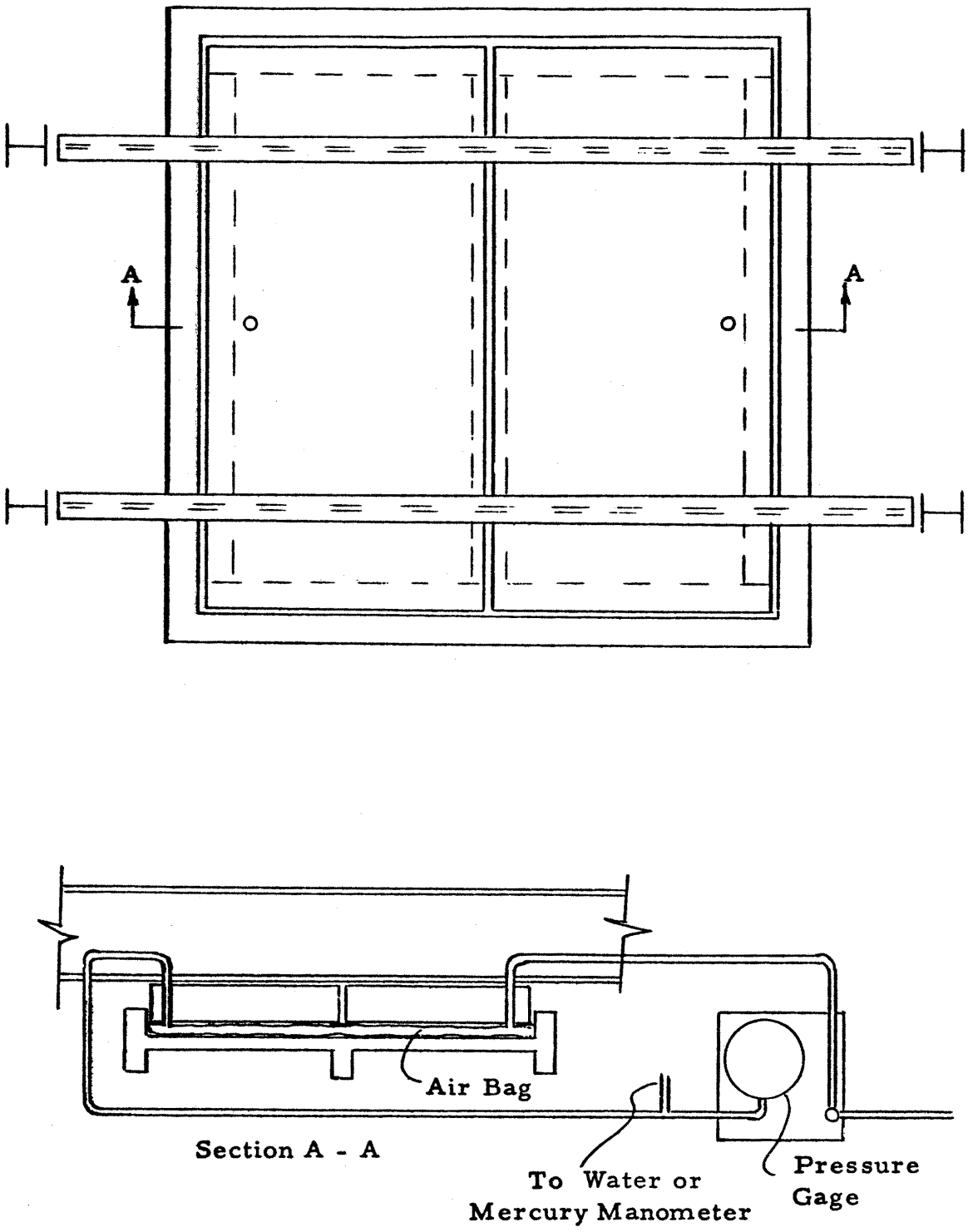


Fig. 2.6. Diagram of Specimen Ready for Test

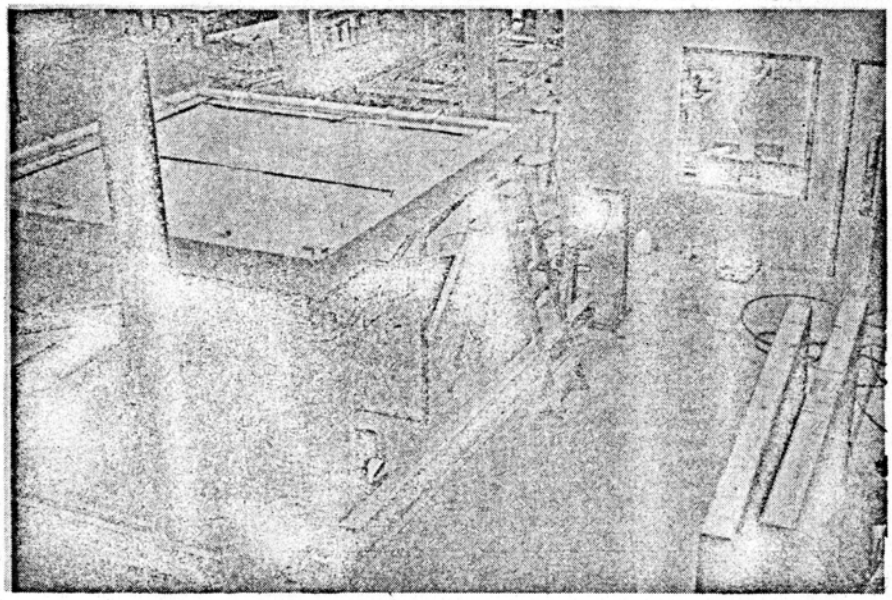

Fig. 2.7. Slab With Bag in Place

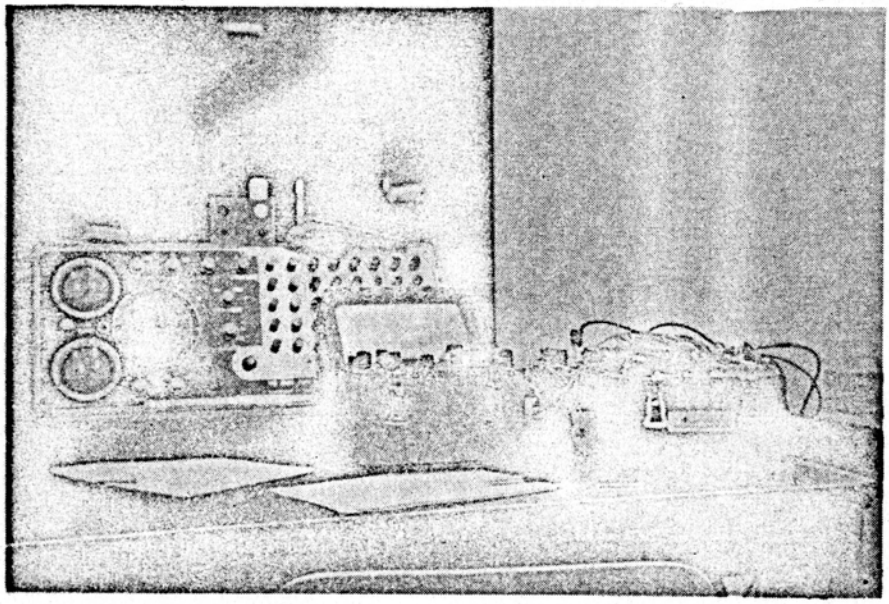

Fig. 2.8. Strain Indicators

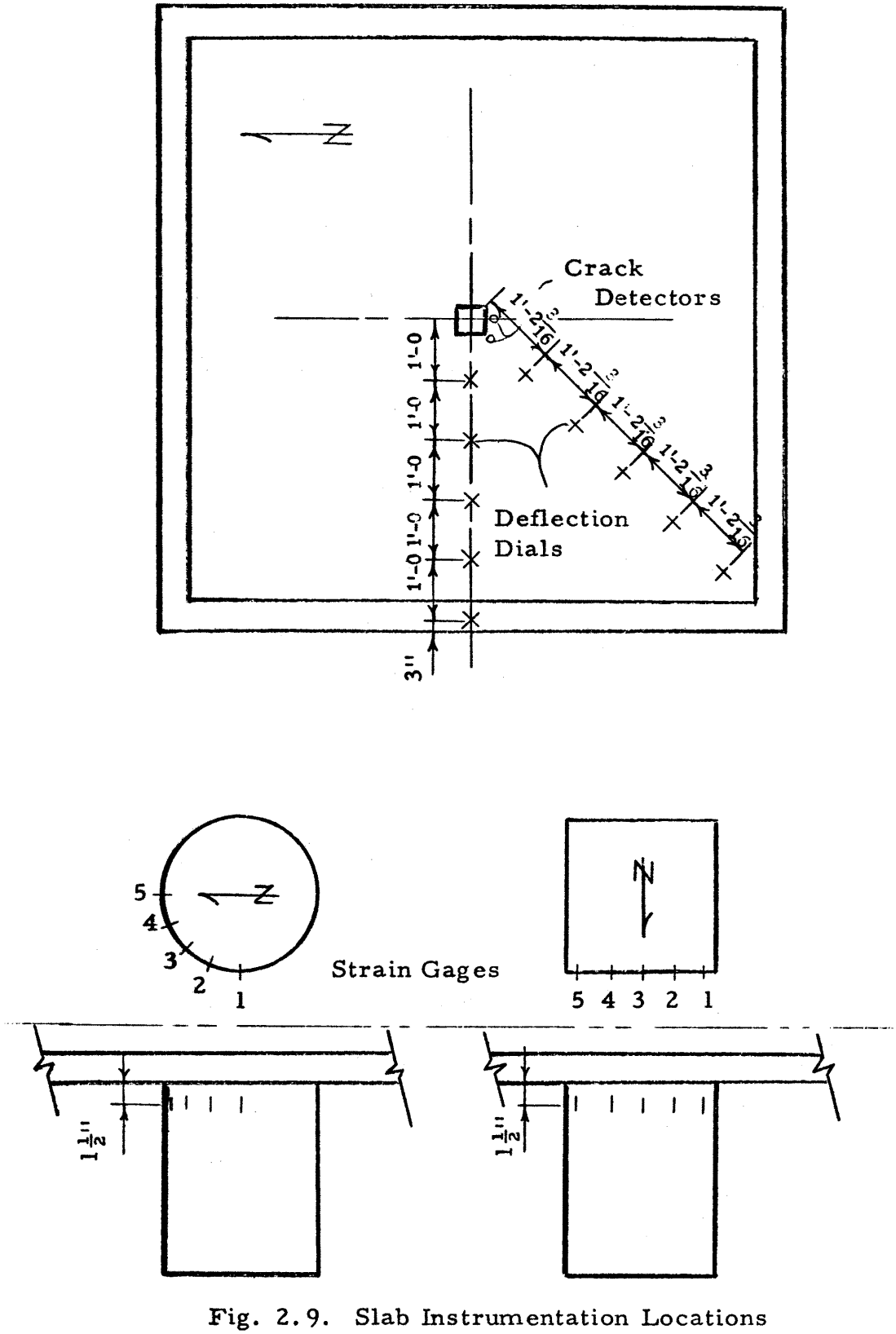


Fig. 2.9. Slab Instrumentation Locations

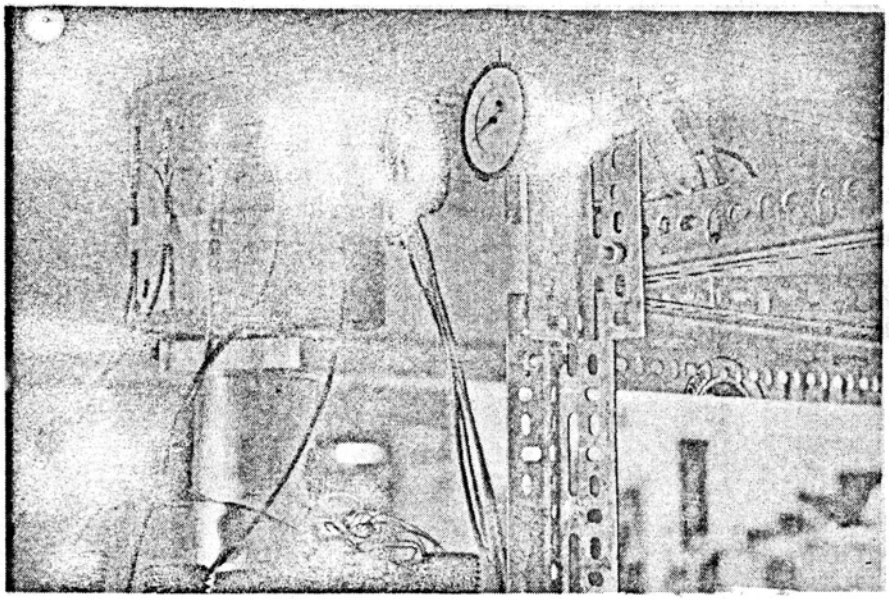

Fig. 2.10. Strain Gage Placement

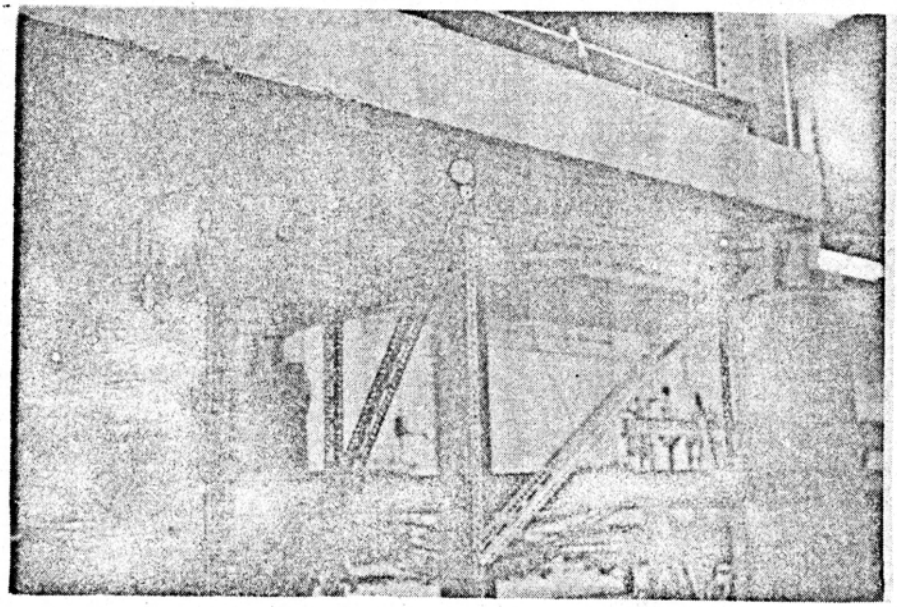

Fig. 2.11. Deflection Dials

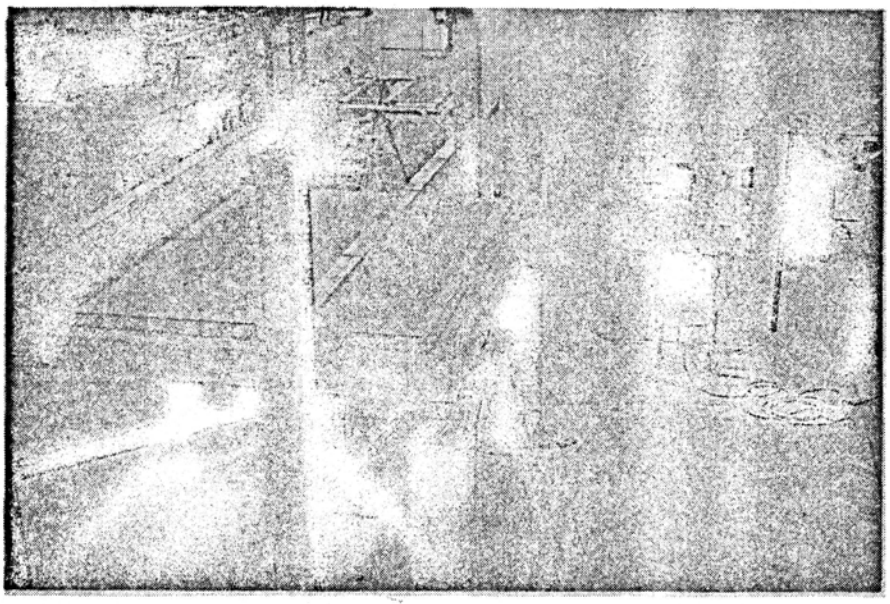

Fig. 2.12. Completed Test Setup

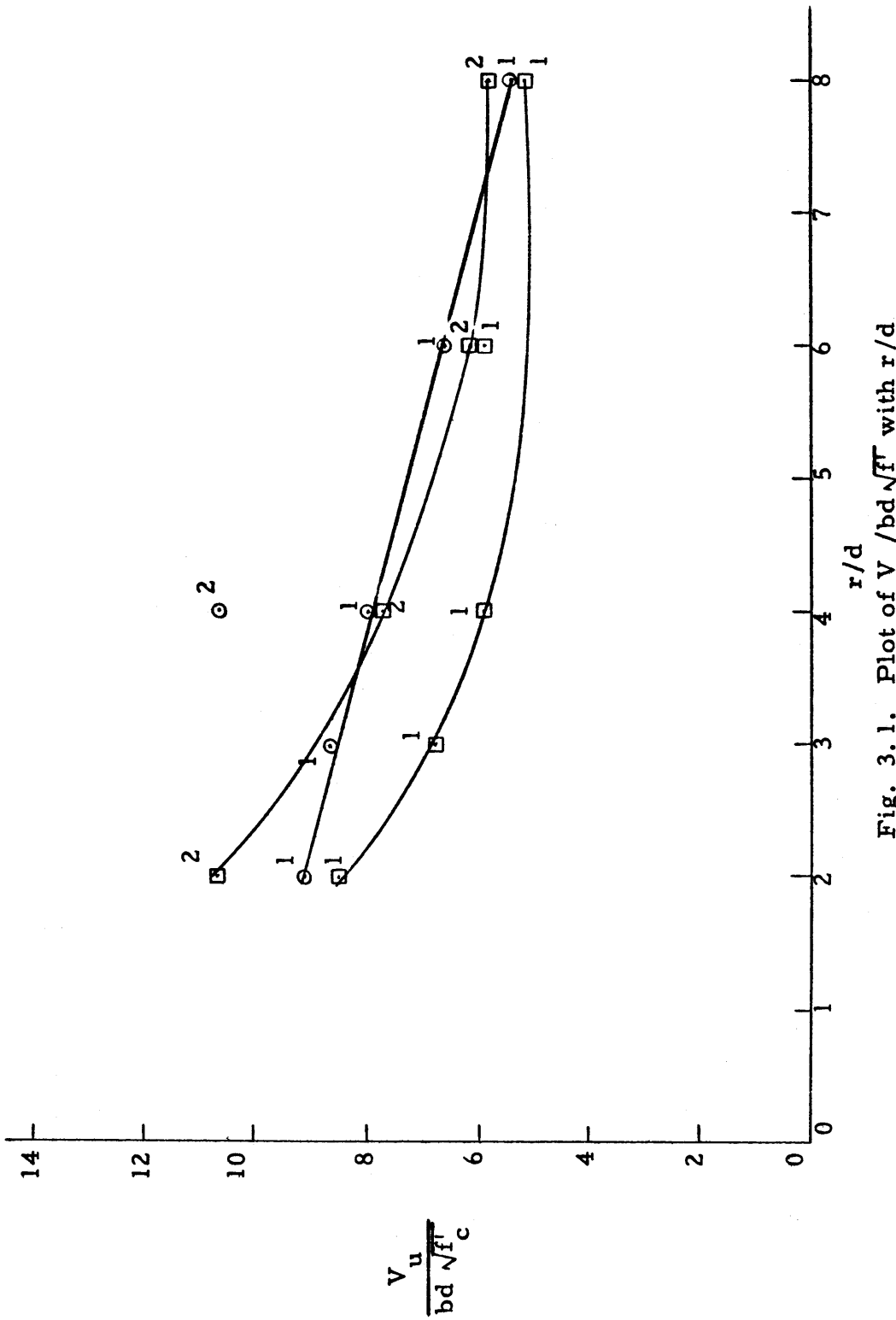


Fig. 3.1. Plot of $V_u/bd\sqrt{f'_c}$ with r/d

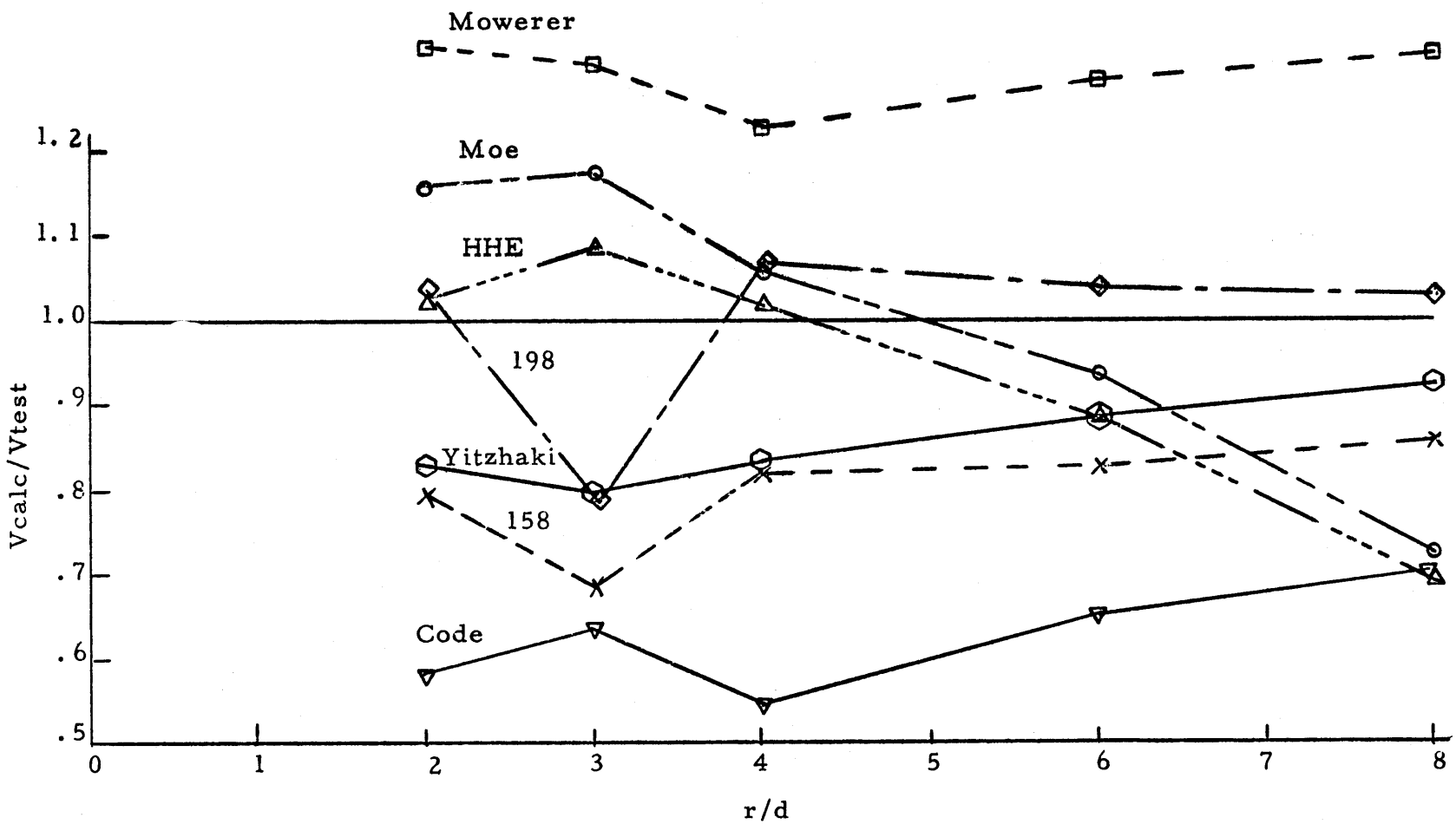


Fig. 3.2. Plot of Average Vcalc/Vtest with r/d

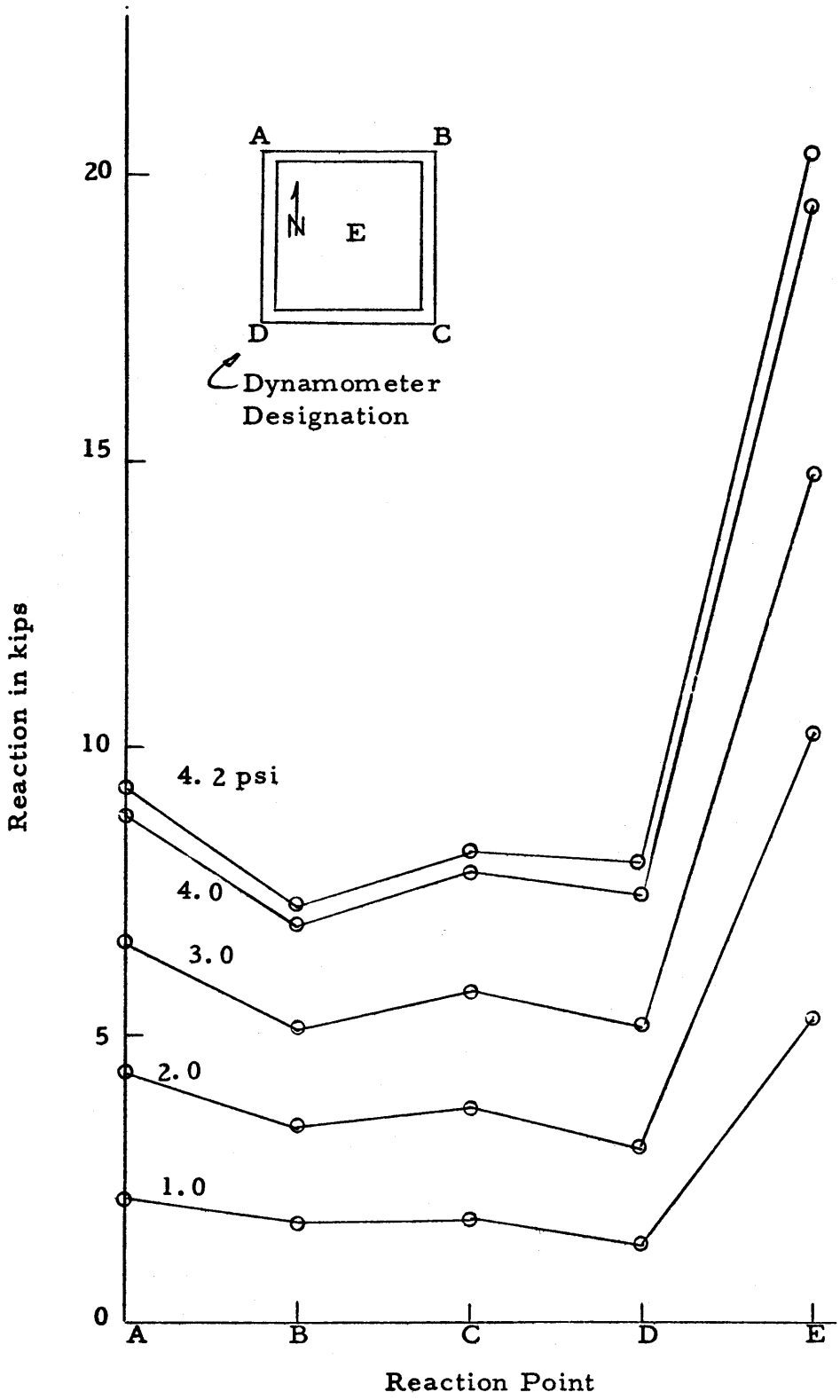


Fig. 4. 1. Vertical Force Reactions for Slab 8S1 - 6

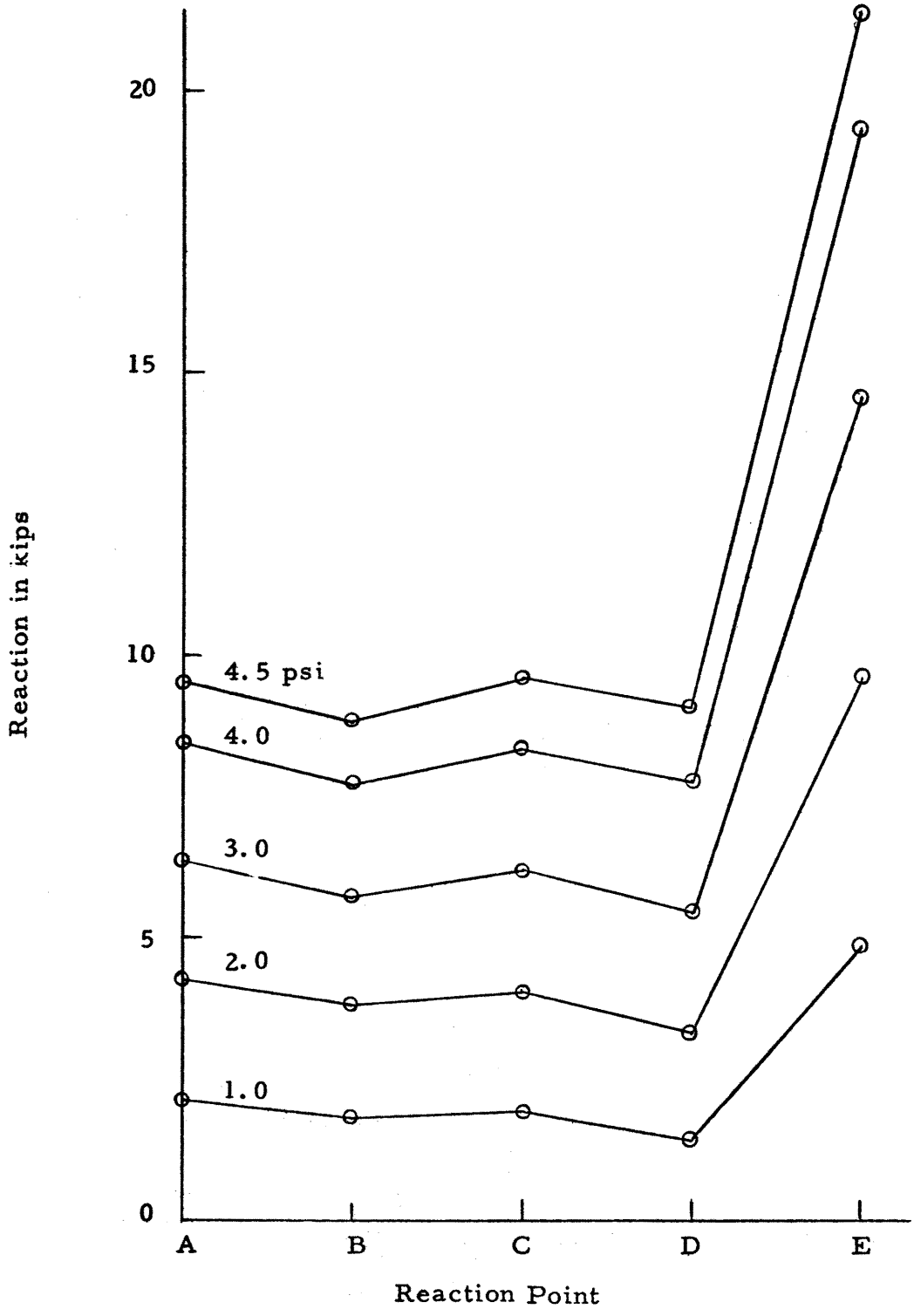


Fig. 4.2. Vertical Force Reactions for Slab 8C1 - 13

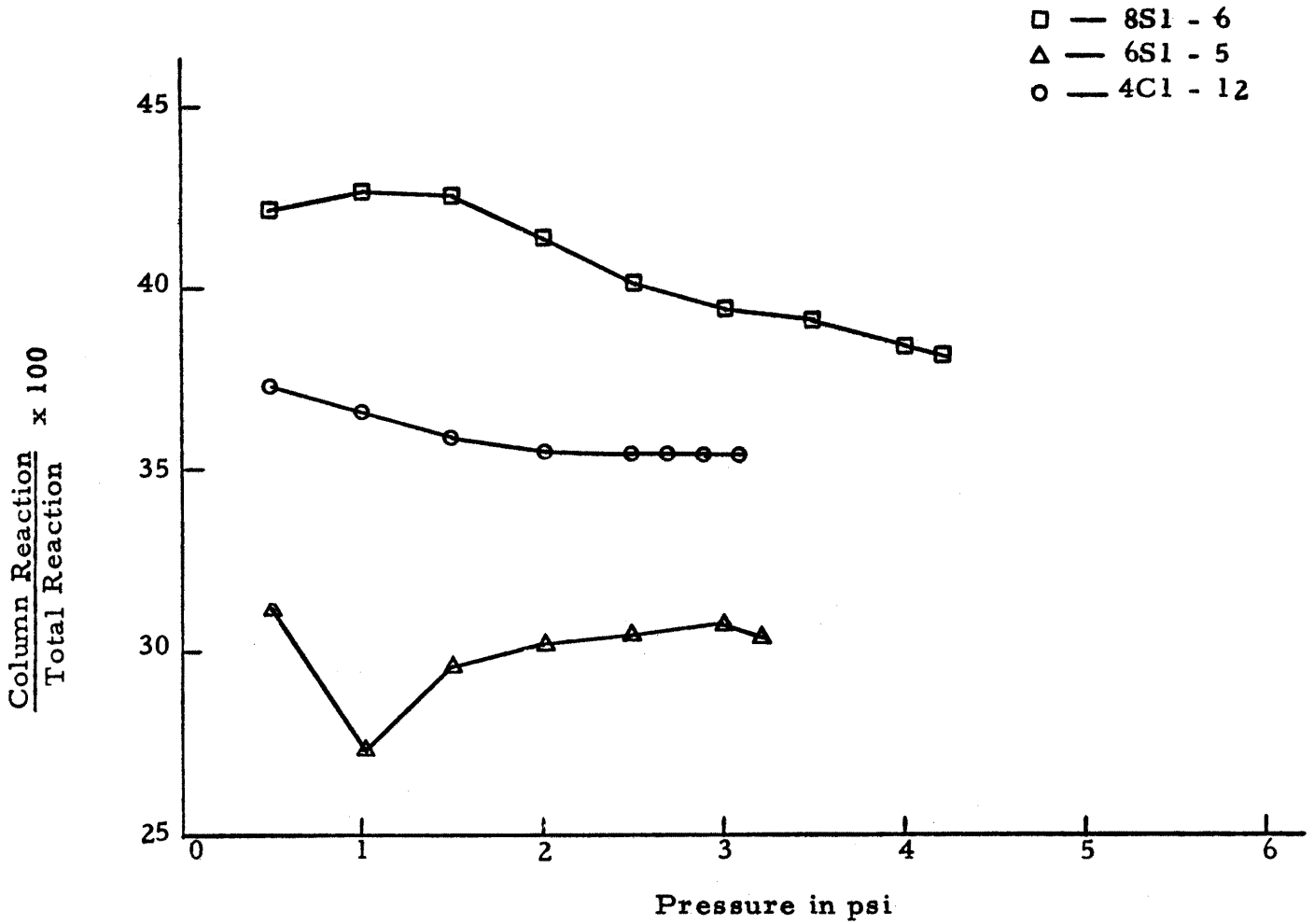


Fig. 4.3. Variation in Column Reaction/Total Reaction with Pressure

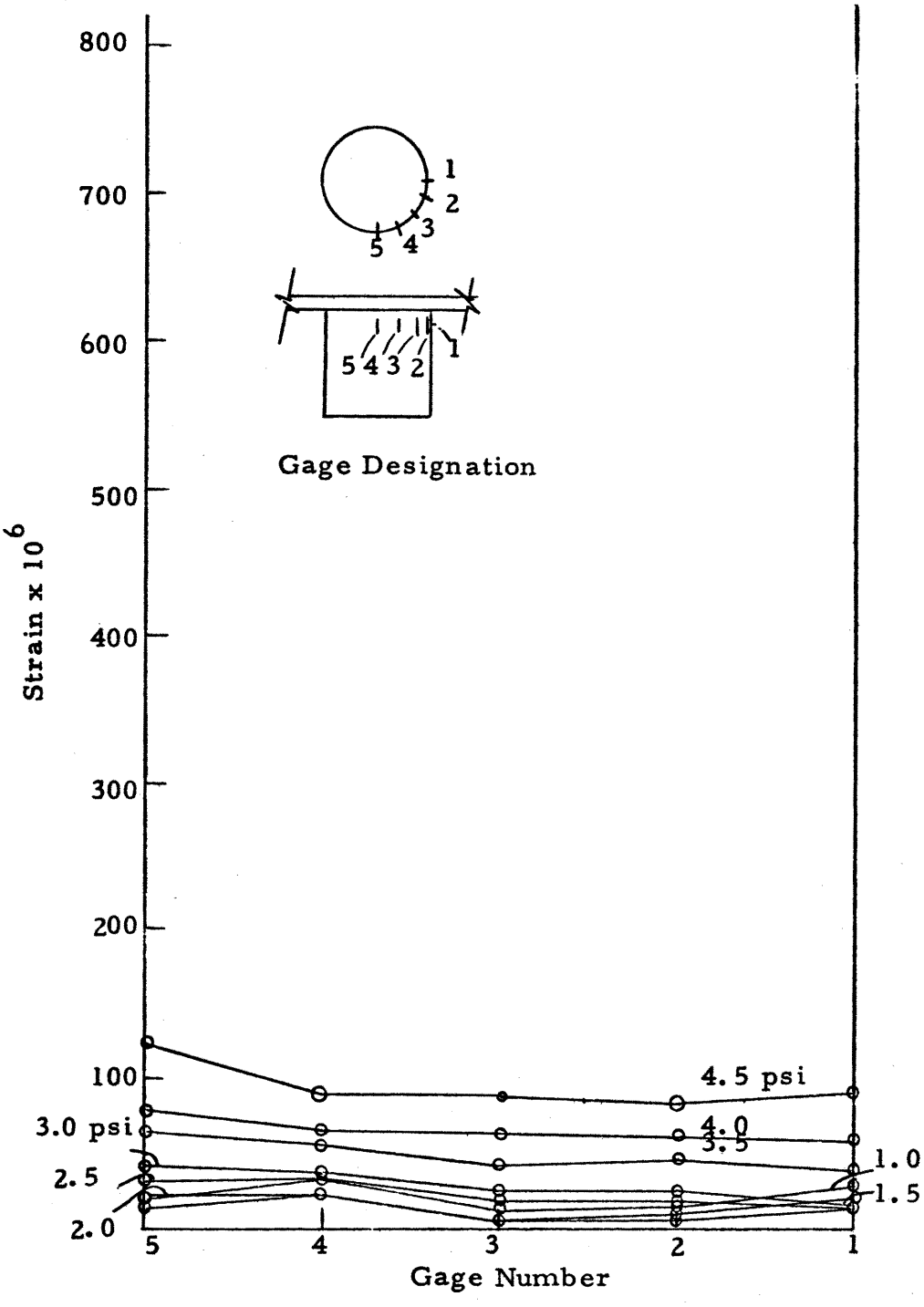


Fig. 4.4. Column Strains for Slab 6C1 - 9

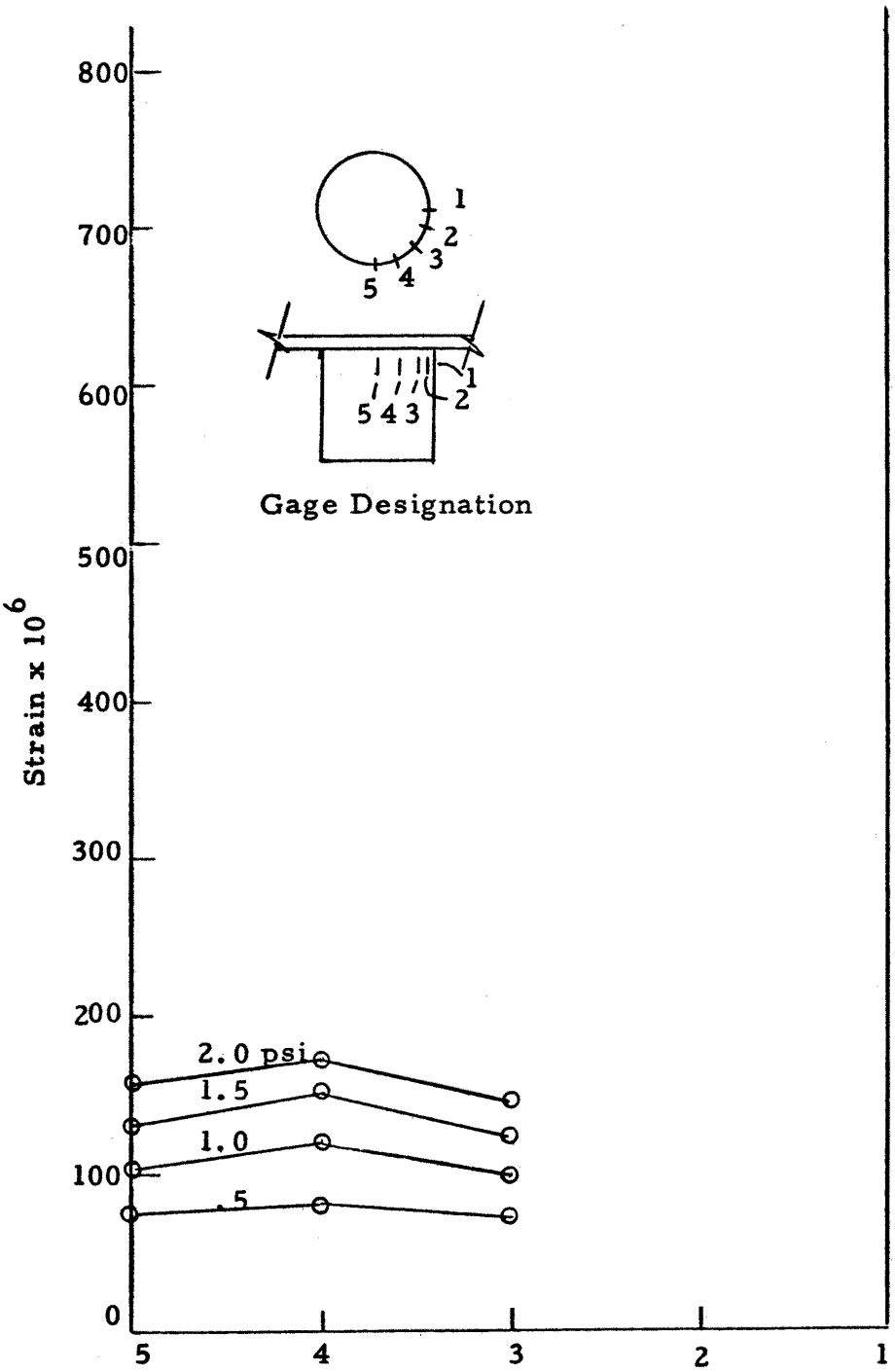


Fig. 4.5. Column Strains for Slab 2C1 - 11

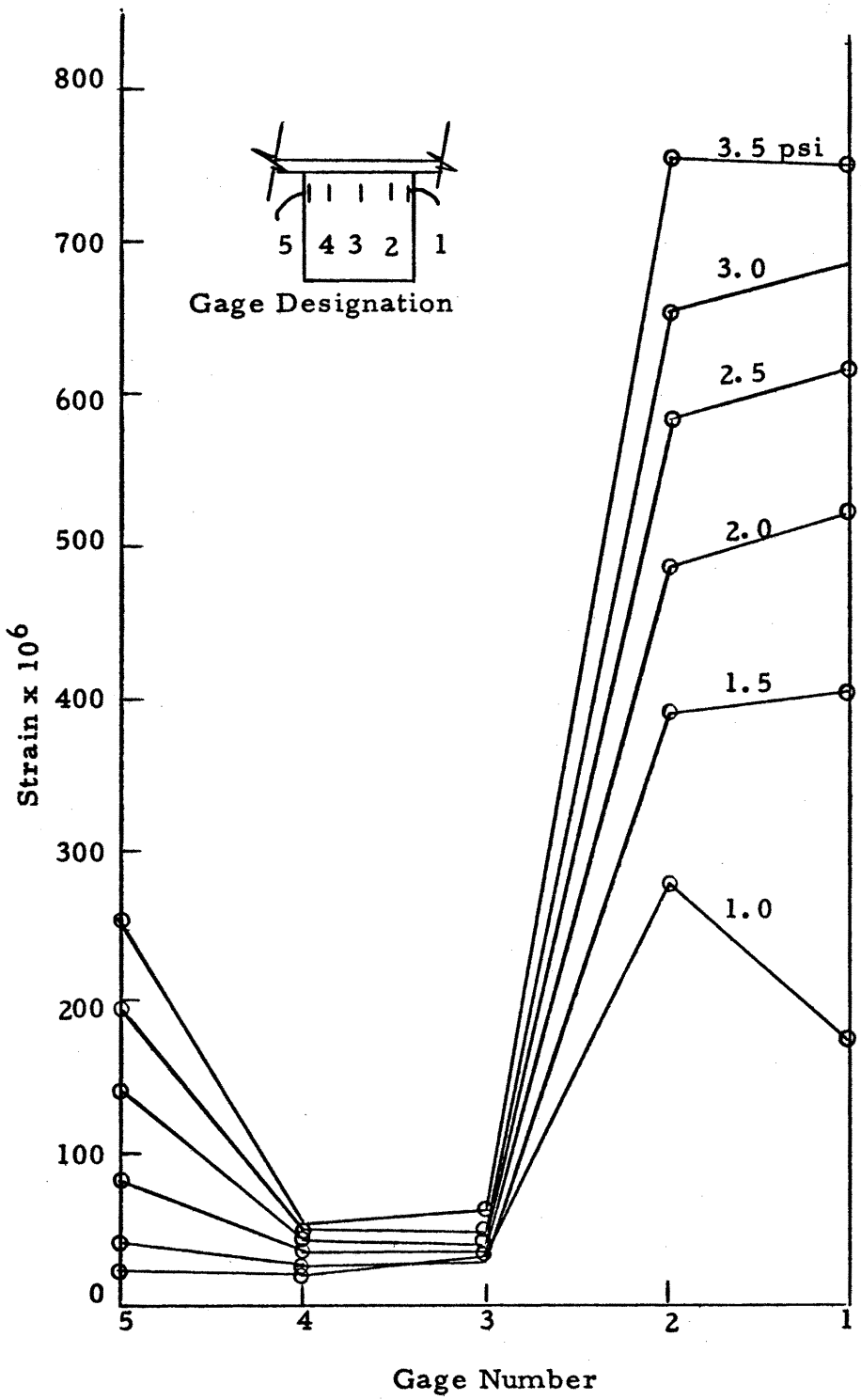


Fig. 4.6. Column Strains for Slab 6S2 - 14

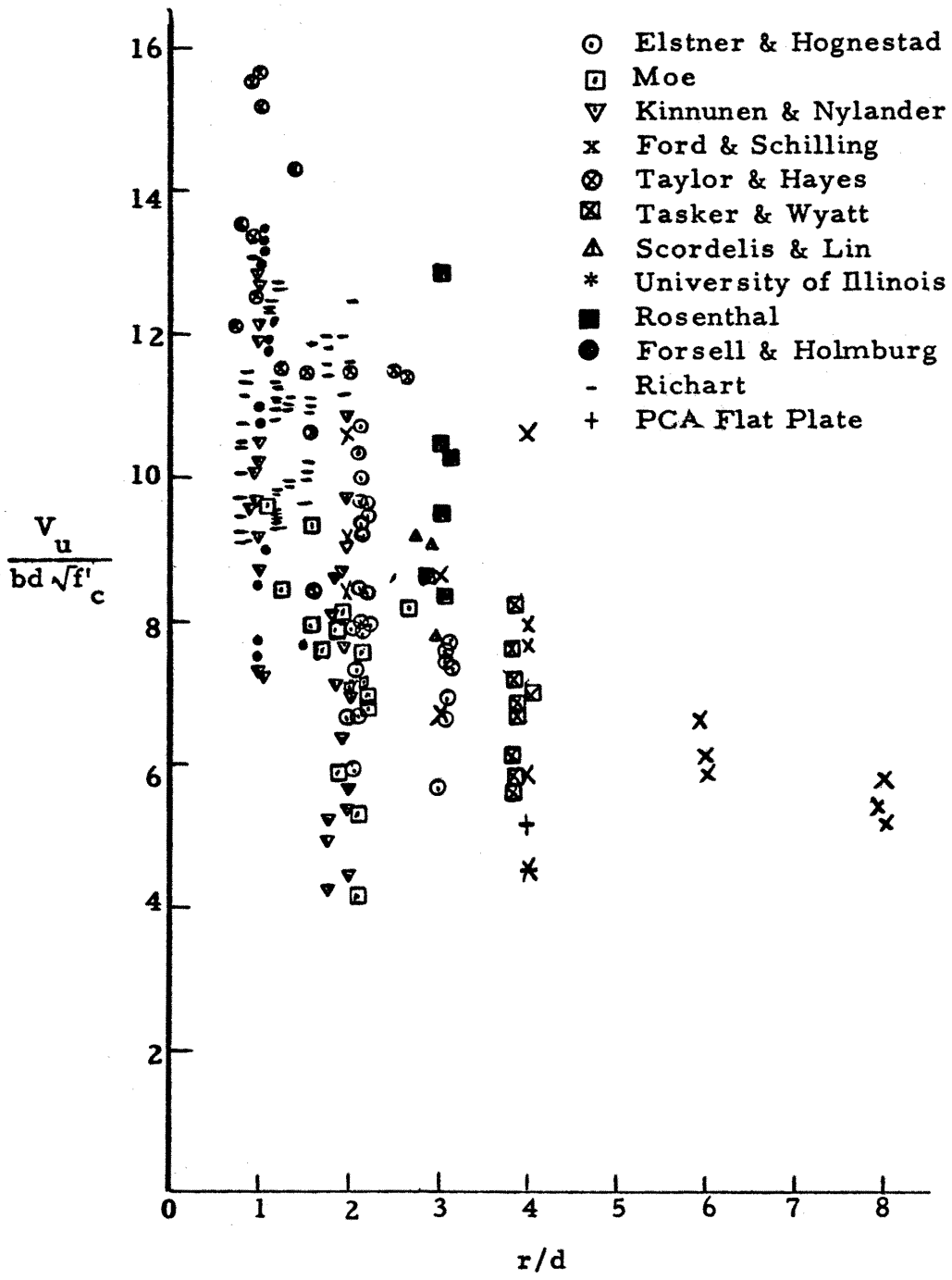


Fig. 4.7. Variation in $V_u/bd\sqrt{f'_c}$ with r/d for Present and Previous Test Series
(from Mowrer (16))

# APPENDIX A

## Dynamometers

Five dynamometers were required to obtain the reaction data for each test. These reaction cells were fabricated from aluminum tubing and plates. The structural shape of the dynamometers is shown in Fig. A. 1. Located in the center of the top plates was a socket which accepted a 1-1/2 inch steel ball which formed an idealized simple support for the test specimens. The tubes were instrumented with electrical resistance strain gages. The strain gages were SR-4 Type A-3-S13 gages with a 2.05 gage factor, 1.0 inch gage length and 120 ohms resistance. The gages were applied with Duco cement.

Two generations of dynamometers were designed. The first generation had a strain gage configuration of three gages mounted at 120 degrees from each other around the tube at mid-height as shown in Fig. A. 1. It was desired to obtain the vertical reaction plus two orthogonal horizontal components. Therefore, with this configuration, a modified flexibility analysis method had to be applied to change strain readings into load readings. The theory used is as follows.

The three reaction components were labeled vertical (V), north (N) and east (E). With the three strain readings as knowns, equation A1 shows the conversion of load to strain.

$$\begin{aligned} a_{11} V + a_{12} N + a_{13} E &= \epsilon_1 \\ a_{21} V + a_{22} N + a_{23} E &= \epsilon_2 \\ a_{31} V + a_{32} N + a_{33} E &= \epsilon_3 \end{aligned} \qquad \text{. - - - A.1}$$

The $a_{ij}$ coefficients were not known and so had to be determined experimentally. Equation A. 1 may be written in matrix form as

$$\begin{bmatrix} a_{11} & a_{12} & a_{13} \\ a_{21} & a_{22} & a_{23} \\ a_{31} & a_{32} & a_{33} \end{bmatrix} \begin{Bmatrix} V \\ N \\ E \end{Bmatrix} = \begin{Bmatrix} \epsilon_1 \\ \epsilon_2 \\ \epsilon_3 \end{Bmatrix} \qquad \text{, - - - A.2}$$

or

$$[A]\{F\} = \{D\} \qquad \text{. - - - A.3}$$

It was desired to calculate F for the strain values obtained from the dynamometers, hence

$$\{F\} = [A]^{-1} \{D\} \qquad \text{. - - - A.4}$$

The A matrix was obtained through loading the reaction cells in the three different directions. To determine vertical calibration a dynamometer was placed standing on its base in a

materials testing machine. To obtain N and E calibrations, a dynamometer was placed in the testing machine at a 90 degree angle to the direction of load application. In this lateral position, the load was applied sequentially in the north, south, east and west directions. The calibration for the north was taken as the average of the north and south and the calibration for the east was taken as the average of the east and west data. The slope of each strain-force curve was placed in the appropriate position of matrix A. The inverse of A was then found so that equation A.4 was satisfied. Strain readings D of the slab test could then be taken and reactions F could be computed using A.4. The first six slabs were tested using these reaction dynamometers.

Fig. A.2 through A.5 show typical plots of the calibration curves for the first generation dynamometers. From these plots some problems with the dynamometers can be detected. For a vertical load in the dynamometer, the slope of the three gages should be identical. Because of the characteristics of the tube and because of the quality of the gages, the slopes of the curves are not equal. The same characteristics are present in the lateral load calibration curves.

Another problem is the fact that the calibration curves did not plot through zero. The gages were zeroed at the beginning of the test so a plot through zero should have resulted since elastic stresses were maintained.

The test results obtained using these dynamometers were not satisfactory as is shown by the plot of the ratio of reaction to load (load = air pressure times area, both correct to about 1%) against pressure in Fig. A. 6. The plot shows instability of the dynamometers for the different tests. The rapid change in the ratio at low pressures can be attributed to the low strain readings produced. The accuracy desired was not obtained with these dynamometers so the second generation dynamometers were produced.

The second generation reaction dynamometers were instrumented with twelve strain gages, 6 active and 6 dummy as shown in Fig. A. 7. The arrangement consisted of three full bridge systems with 2 active and 2 dummy gages per bridge as shown in Fig. A. 8. One bridge was used to measure vertical loads while the other two bridges measured lateral loads. The second generation dynamometers had Micro-measurement Bakelite, foil gages with 2.06 gage factor, 120 ohm resistance and 0.5" length. The gages were mounted with a special adhesive which required baking to cure.

The active gages in the bridges were arranged so as to read only the effect desired. In order to read vertical reaction only, the active gages were located on opposite sides of the bridge. In this manner the bridge should cancel any bending effect. For the horizontal reactions the active gages were located on adjacent sides of the bridge. In this way the bridge should cancel any vertical effect.

Calibration of the second generation cells was done in the same manner as the first generation. With this system the calibration curves could be used directly to compute load readings.

Fig. A.9 and A. 10 show typical calibration curves for the second generation dynamometers. Since the strains were taken on opposite sides of the dynamometers, a better average of strain was obtained over the cross-section than was obtained for generation one dynamometers. The gages used were of much improved quality than existed on the first generation load cells. With these improvements good calibrations were obtained. The curves plotted through zero and the east and north calibrations were nearly equal for the individual dynamometers as should have been the case.

Better results were obtained with these dynamometers as can be seen by the plot of the ratio of reaction to load against pressure in Fig. A. 11. The plot shows results within the limits desired at the ultimate failure load region. Also, the stability of the second generation dynamometers is greater than the first generation dynamometers as can be seen by comparing Fig. A. 5 and A. 11.

Figure A. 12 shows the horizontal reactions of the five reaction dynamometers for the test 6S2 - 14. The reactions shown are typical for all the test specimens. All reactions at the corners were in directions away from the slabs showing rotational effects

that were present in the spandrel beams. The center dynamometer shows that there was some lateral load on the column, thus the column did not punch through with pure normal forces present. This was typical for other test specimens also. The center dynamometers for most slabs showed somewhat the same maximum lateral force of about 500 pounds. Two specimens showed a lateral force at the column of over 1000 pounds. Test 4S2 - 8 showed a maximum lateral reaction of 1236 pounds. The resulting moment of 7.6 inch-kips existed at the column connection with the slab, but because of the magnitude of the vertical load, the resulting eccentricity was only .53 inches. The maximum eccentricity of .57 inches was observed in slab 4C2 - 15. The moments in the columns did not seem to cause any of the strength discrepencies found in the test.

Fig. A. 12 shows that the sums of the lateral reactions are not equal to zero as was expected. The percent of the resultant lateral reaction compared to the total vertical reactions is shown in Fig. A. 12 to be less than one percent. None of the other slabs showed a resultant lateral reaction greater than one percent of the total vertical reaction. Unequal load distributions by the air bag against the spandrel beams might have been the cause of this imbalance.

On the whole, the signs of the resultant lateral reactions did not change for any one particular slab though the signs might be different for different slabs. In other words, the lateral load resultants were always in constant directions.

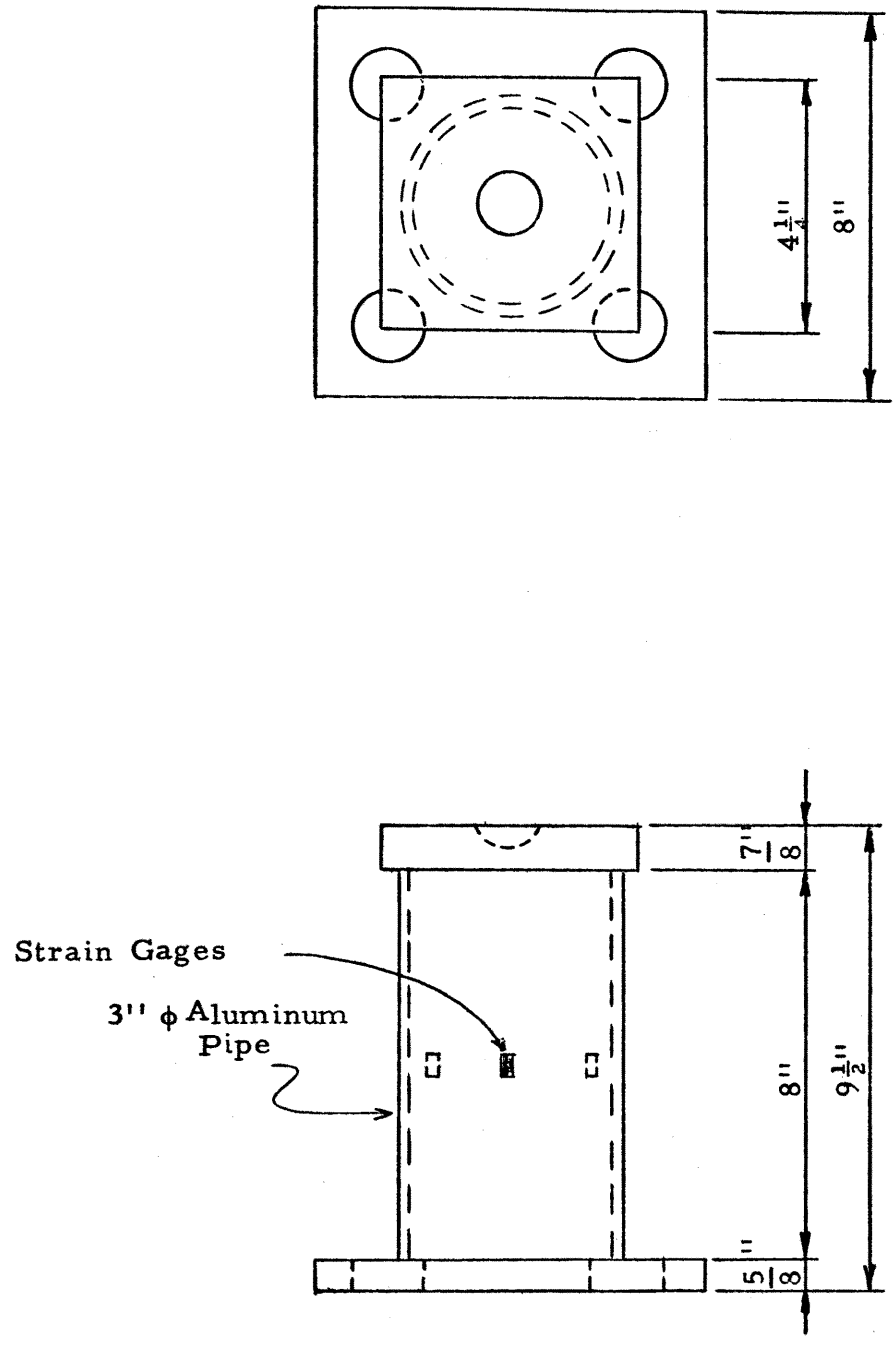


Fig. A. 1. First Generation Dynamometer

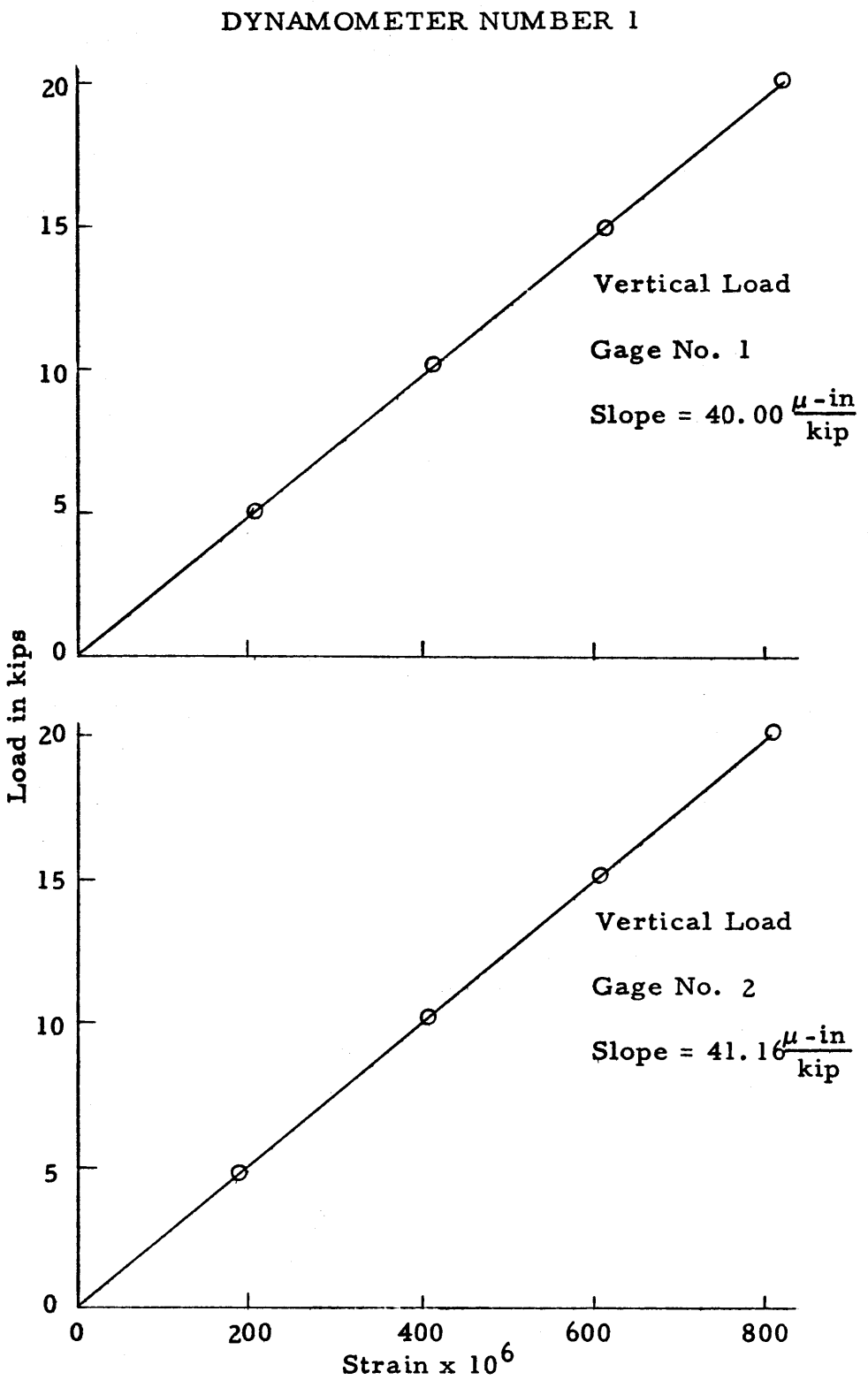


Fig. A. 2. Calibration Curve for First Generation Dynamometer

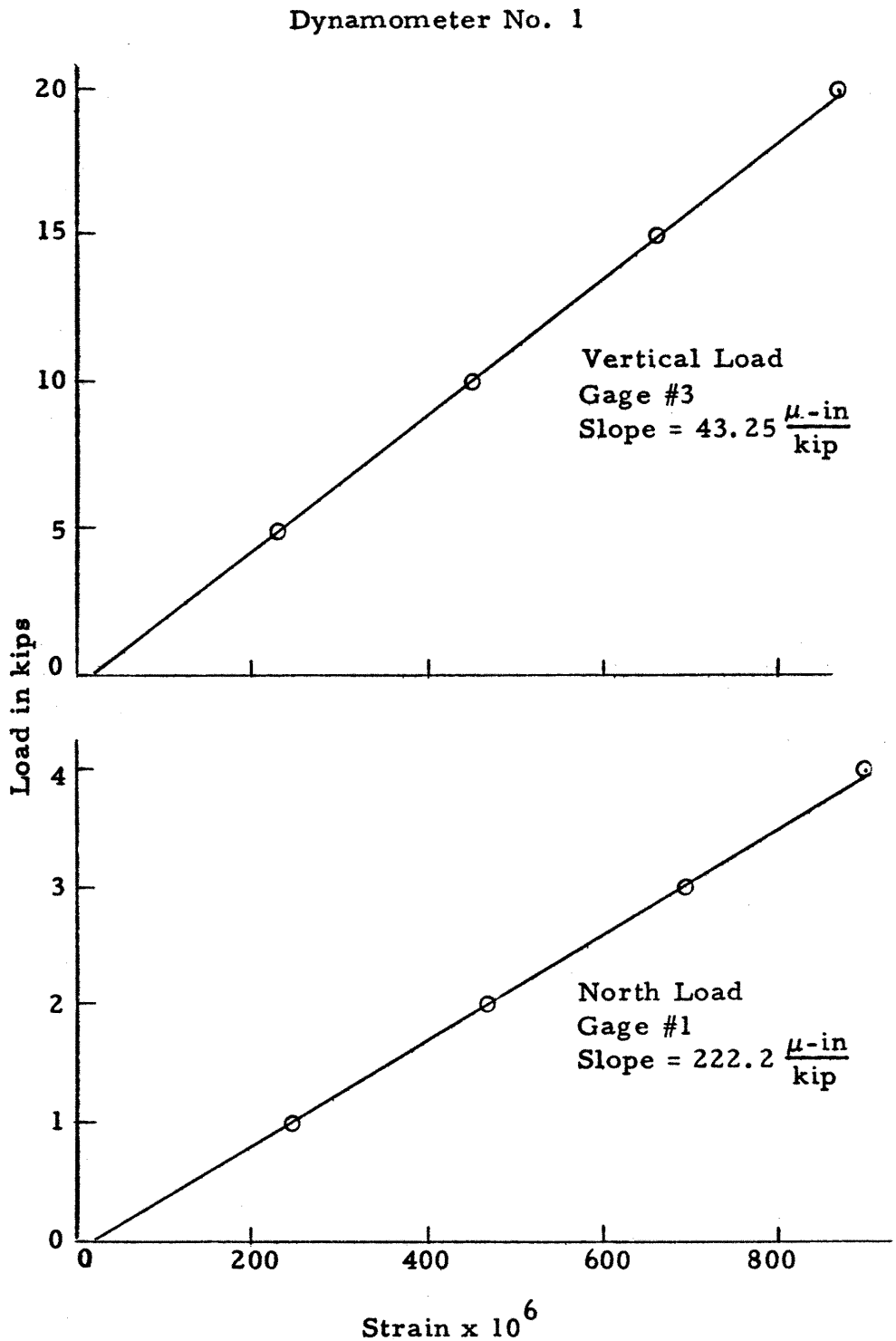


Fig. A. 3. Calibration Curve for First Generation Dynamometer

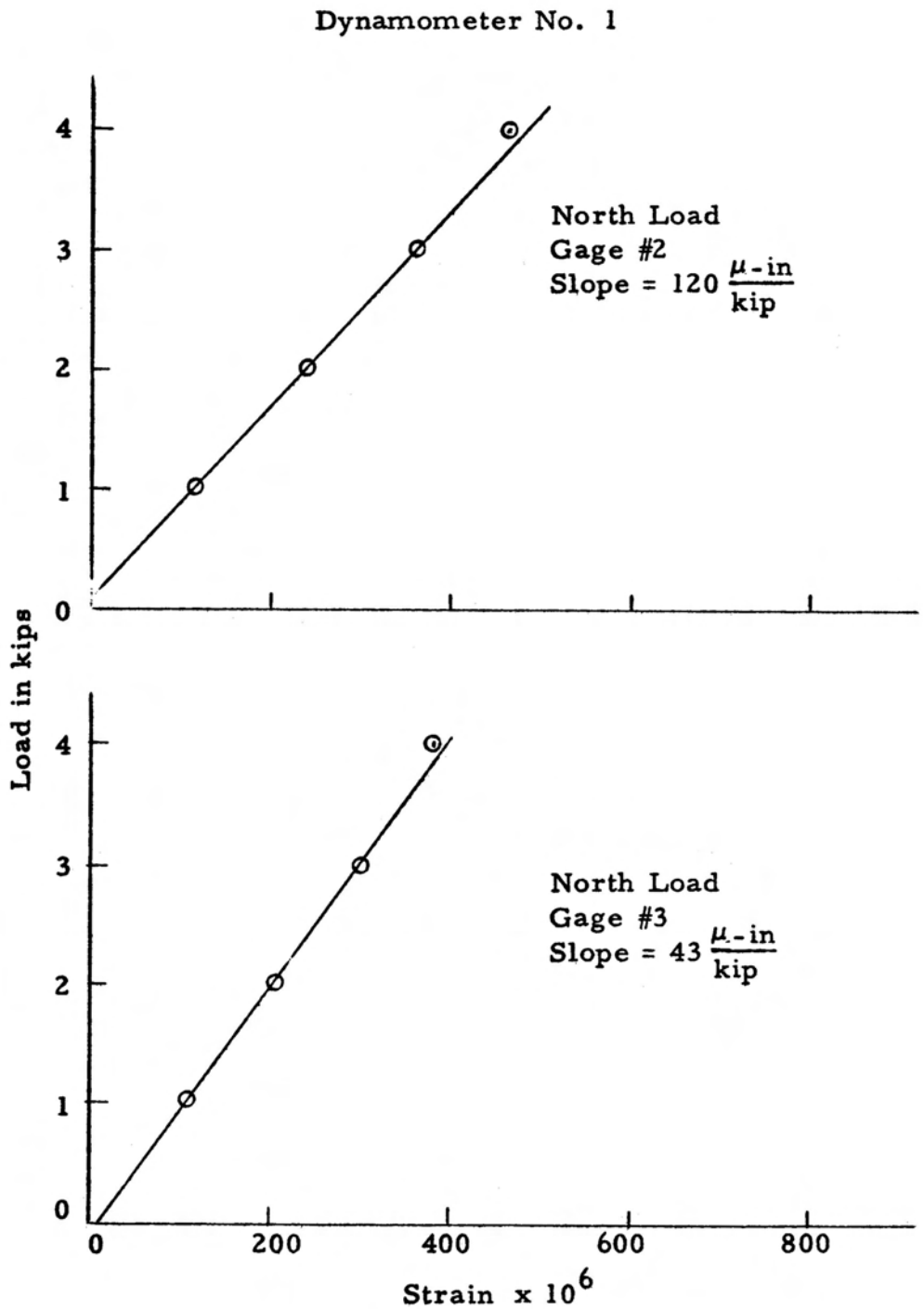


Fig. A.4. Calibration Curve for First Generation Dynamometer

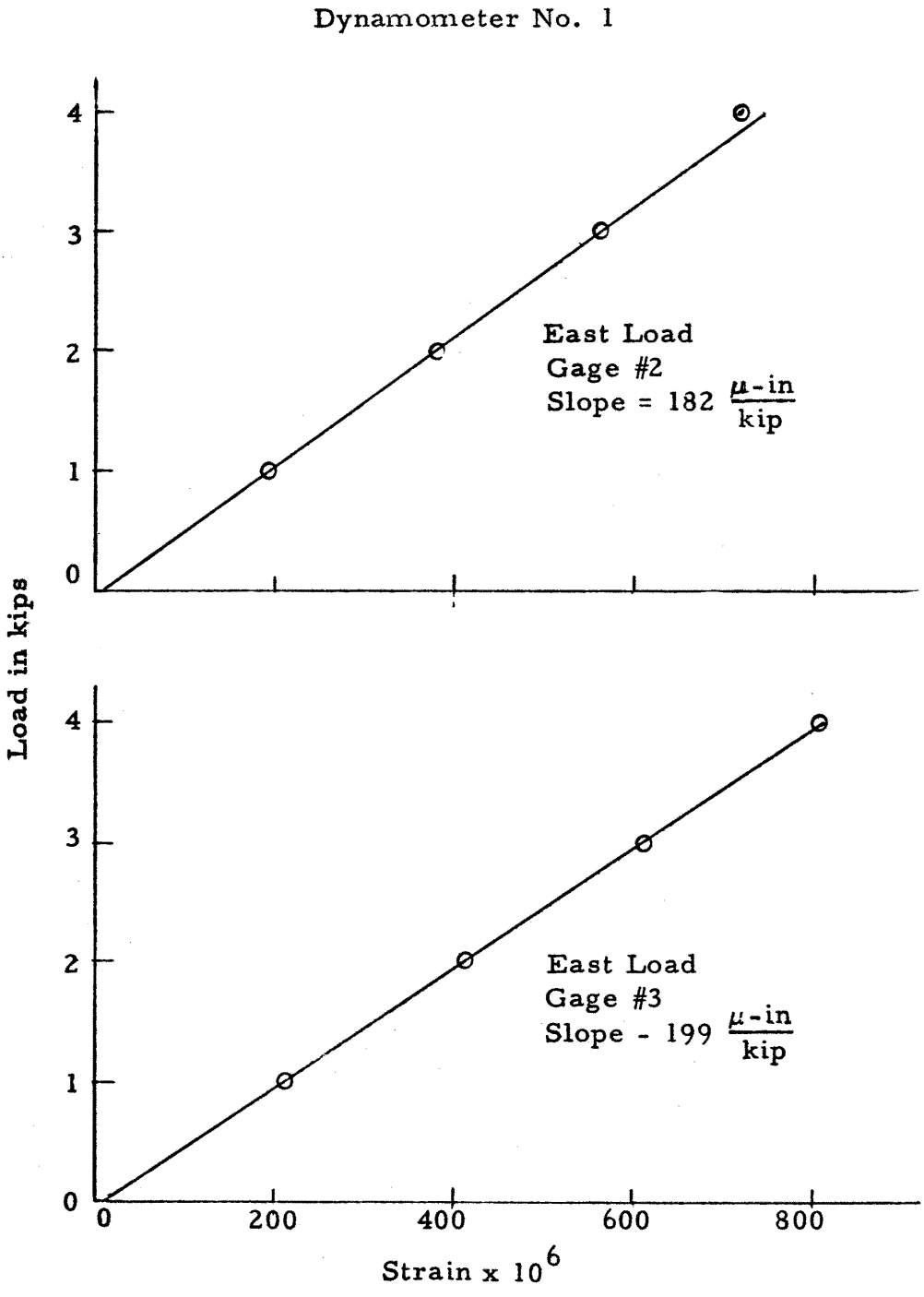


Fig. A. 5. Calibration Curve for First Generation Dynamometer

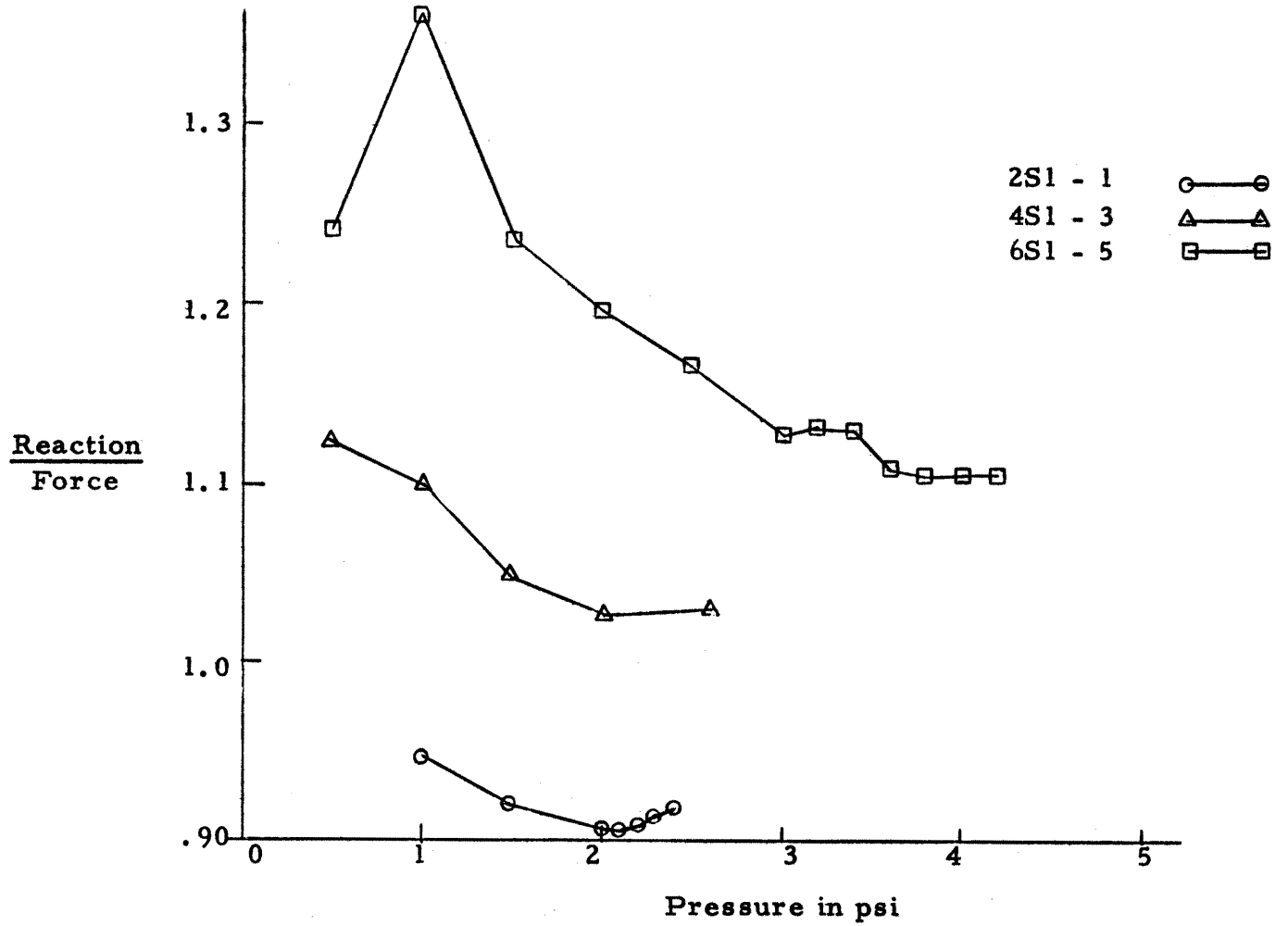


Fig. A. 6. Variation of Reaction/Load with Pressure for Three Tests With Generation One Dynamometers

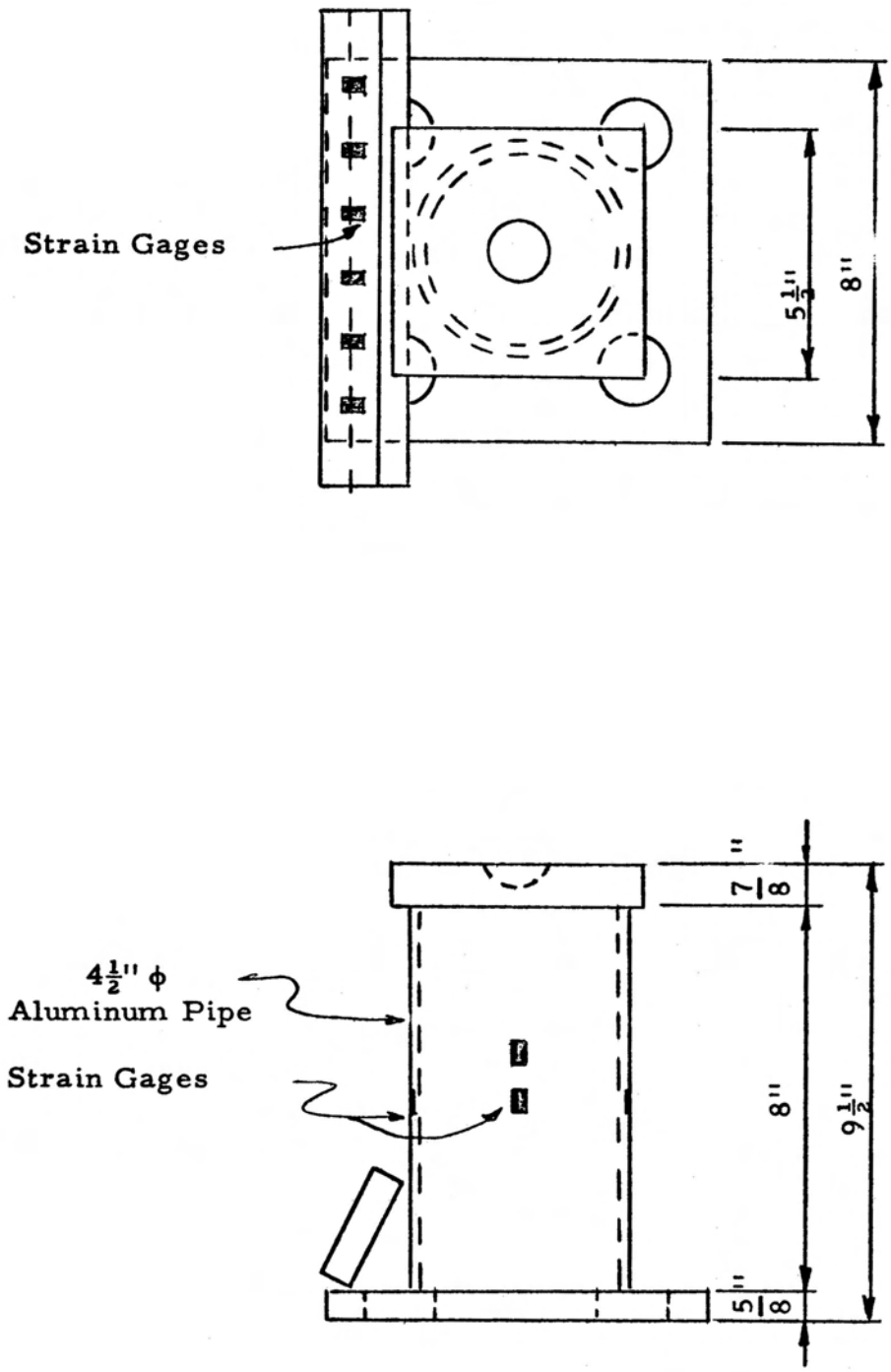


Fig. A. 7. Second Generation Dynamometer

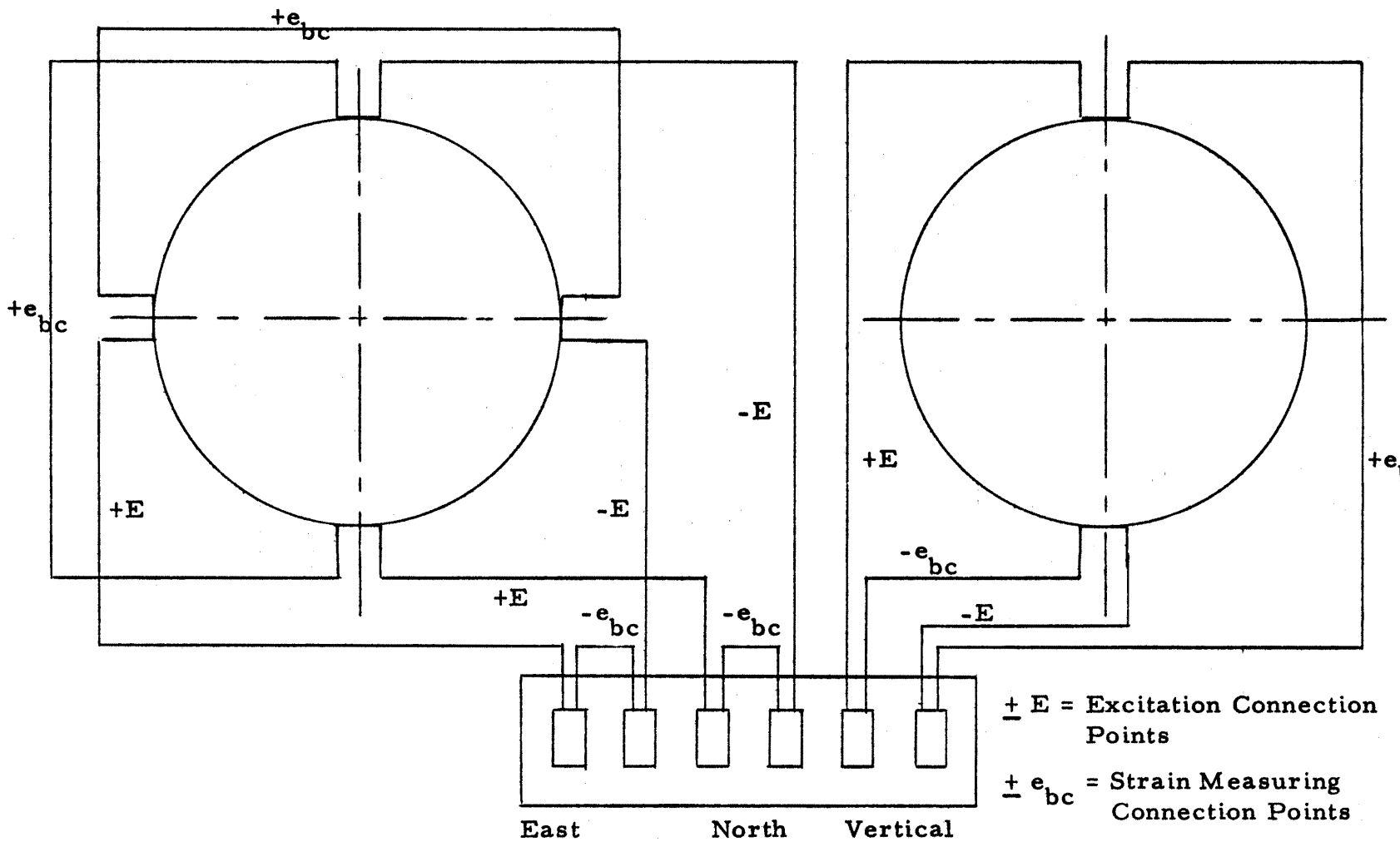


Fig. A.8. Second Generation Dynamometer Wiring Diagram

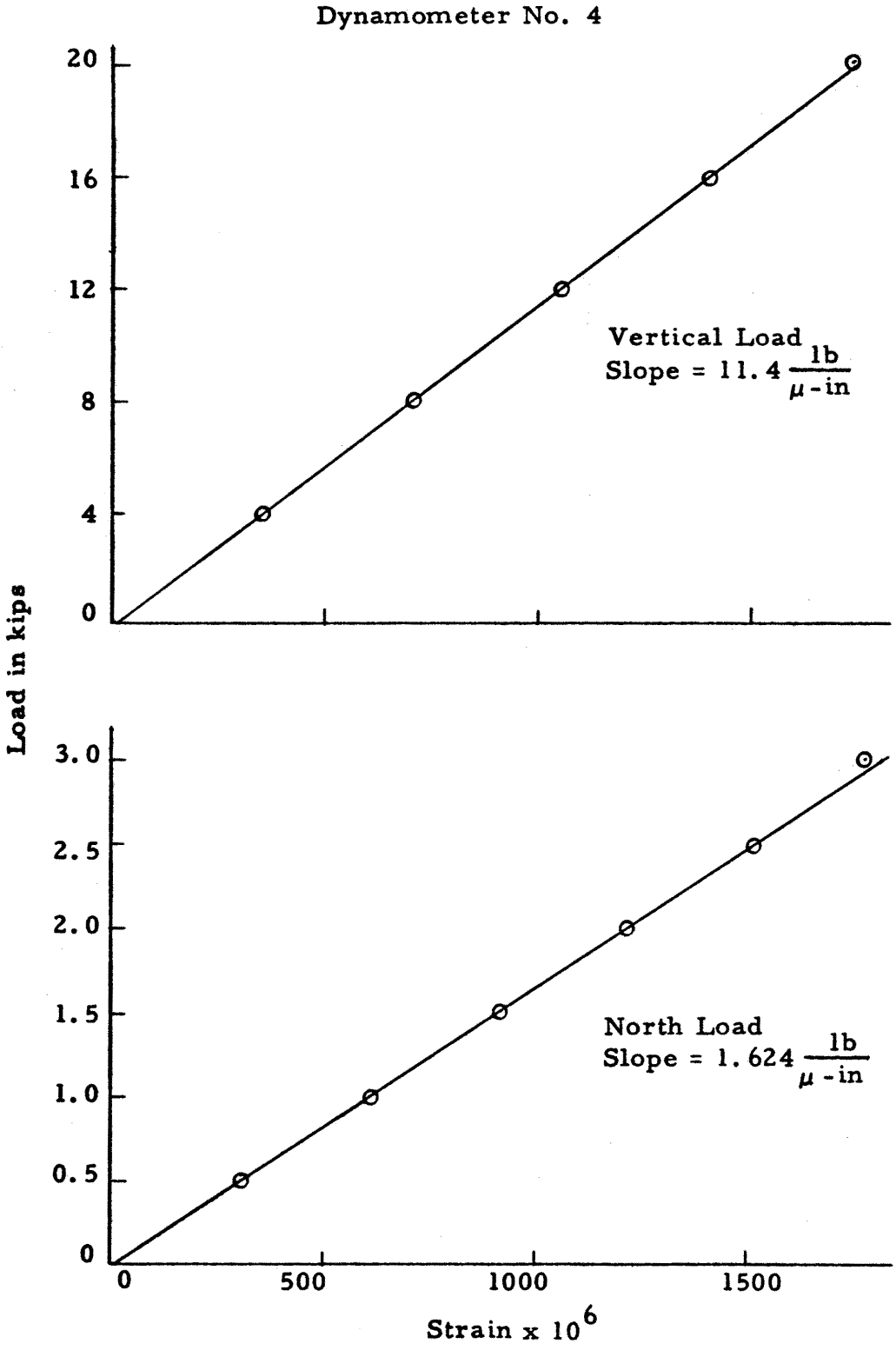


Fig. A.9. Calibration Curve for Second Generation Dynamometer

Dynamometer No. 4

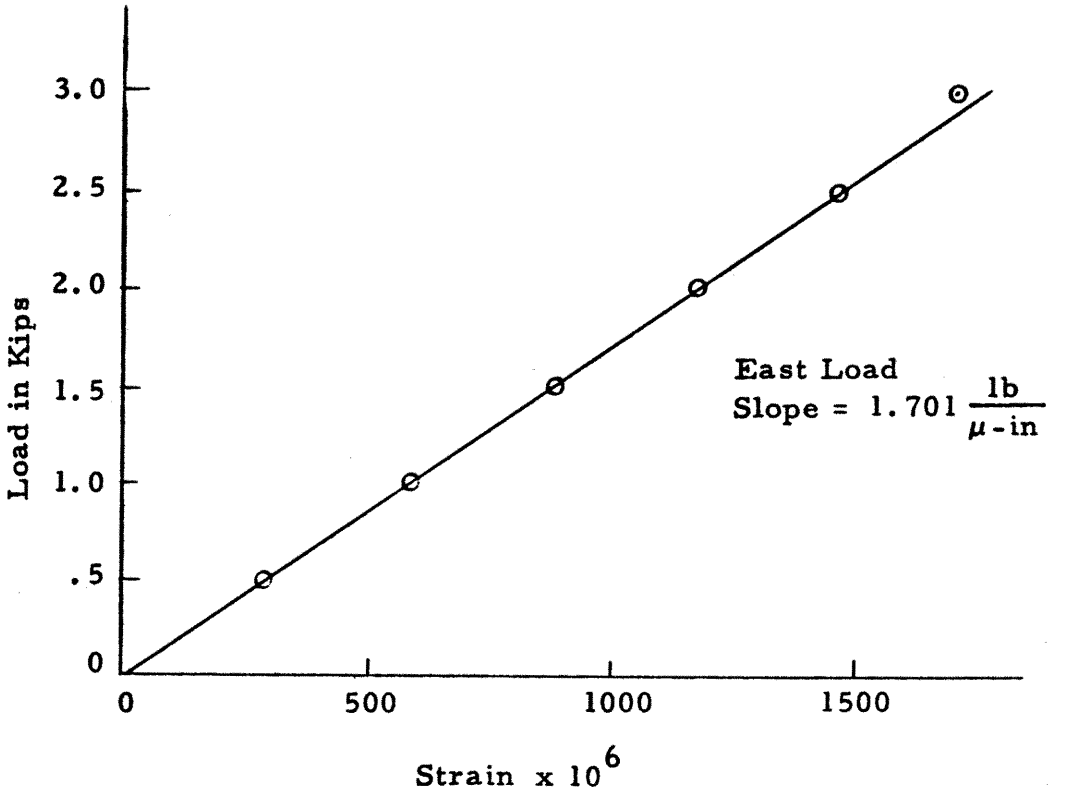


Fig. A. 10. Calibration Curve for Second Generation Dynamometer

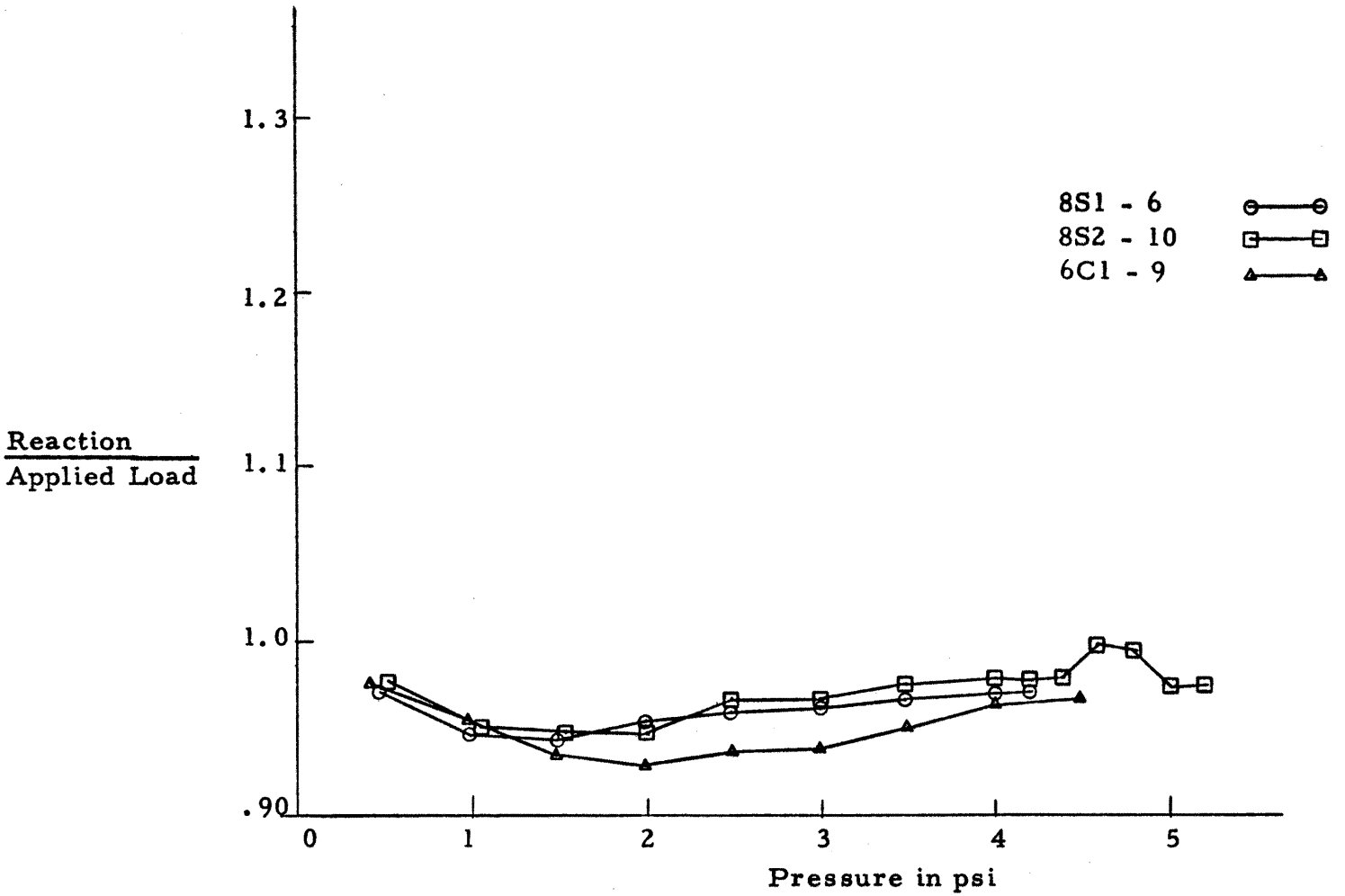


Fig. A. 11. Variation of Reaction/Load with Pressure for Three Tests with Generation Two Dynamometers

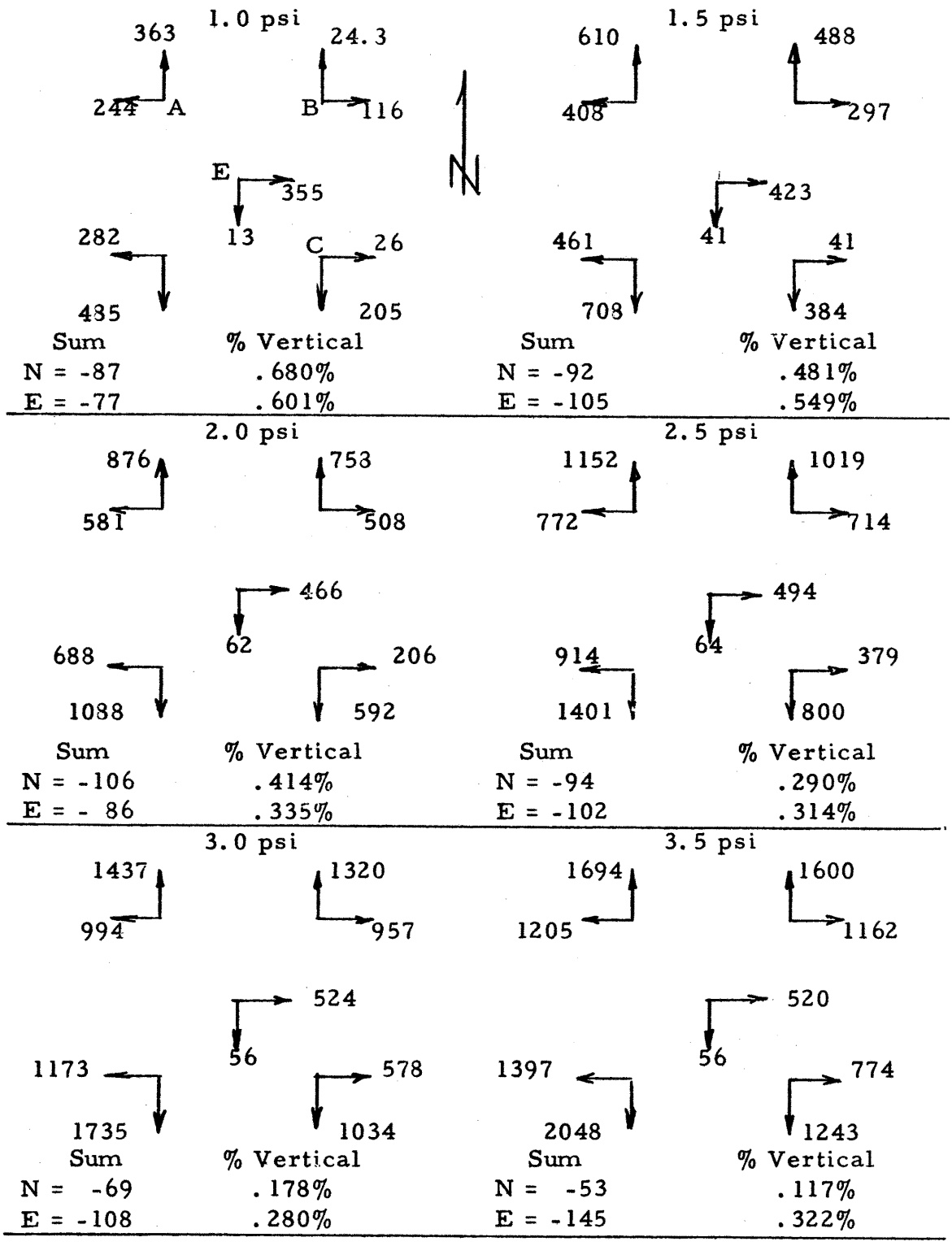


Fig. A. 12. Horizontal Reactions for Test 6S2-14 in Pounds

# APPENDIX B

## Crack Detectors

The crack detectors were used to determine when the shear crack initially opened at the column periphery. There were two of these devices in service which were placed one inch away from the column adjacent to the south side and the southwest corner of the slab as shown in Fig. 2.9.

The crack detectors were made of aluminum rings three inches in diameter and 3/4 inch wide as shown in Fig. B.1. Two holes 3/8 inch in diameter were located 180 degrees apart so that a steel rod could fit through the ring. Four electrical resistance strain gages were placed on the rings 90 degrees from the holes. The gages were mounted both on the inside and outside of the ring and were connected in a full bridge system. Pressure on the ring in the direction of the axis of the rod would produce a resulting strain in the gages.

When the slabs were cast, 1/4 inch diameter holes were made near the column to receive the steel rod when the tests were performed. A wood cap was connected to the top of the rod with plastic wood. This cap acted as a fail-safe device so that the crack detectors were not crushed when the slab failed. A tin box was

placed over the cap so that pressure from the air bag would not affect the reading of the crack detectors. When the crack detectors were placed on the slab, the nuts on the rods were tightened to give an initial strain so that any thinning of the cross section could be monitored; see Fig. B.2.

Crack detector results from three slabs are presented in Fig. B.3, B.4 and B.5. The points of abrupt change in strain readings can be considered the points at which the shear cracks formed. From the data obtained, there can be no general load value assigned as to when the cracks opened for all slabs tested. In general, the cracks opened at loads above 50% of the ultimate load.

In some of the tests, one or both of the crack detectors showed an increase in their diameters with increasing load until the shear crack formed. This meant that the slab was thinning out during the test. The particular strain readings were very small so this effect could be attributed to Poisson effects or drift of zero balance in the gage systems.

The results of the crack detectors are of a qualitative nature because of difficulty in calibration of the devices.

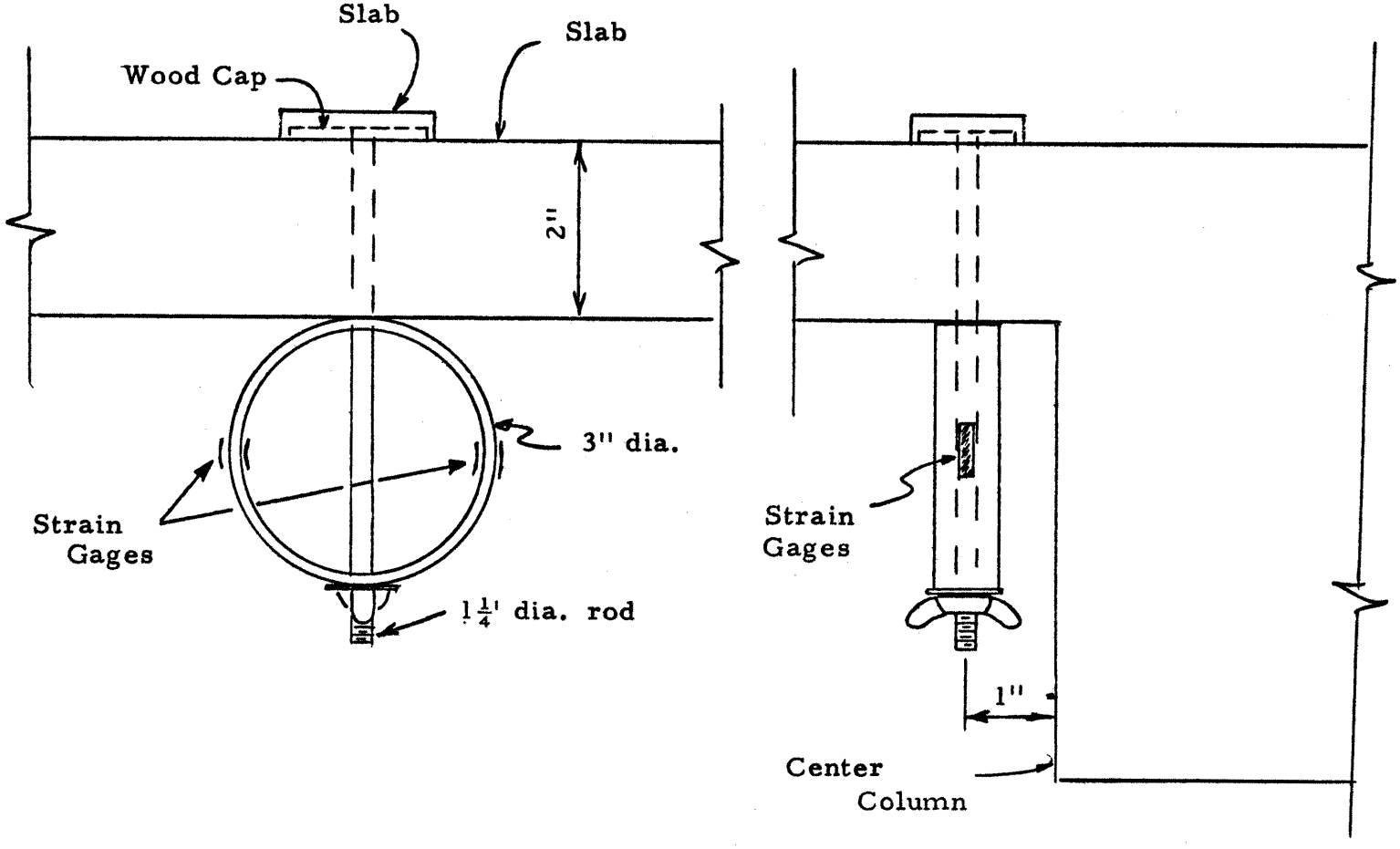


Fig. B. 1. Crack Detector

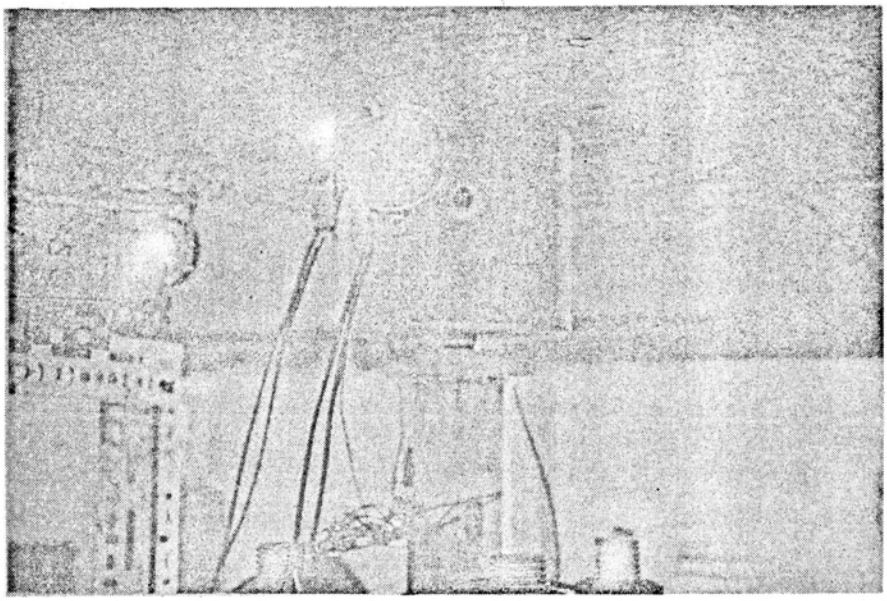

Fig. B.2. Crack Detector Placement

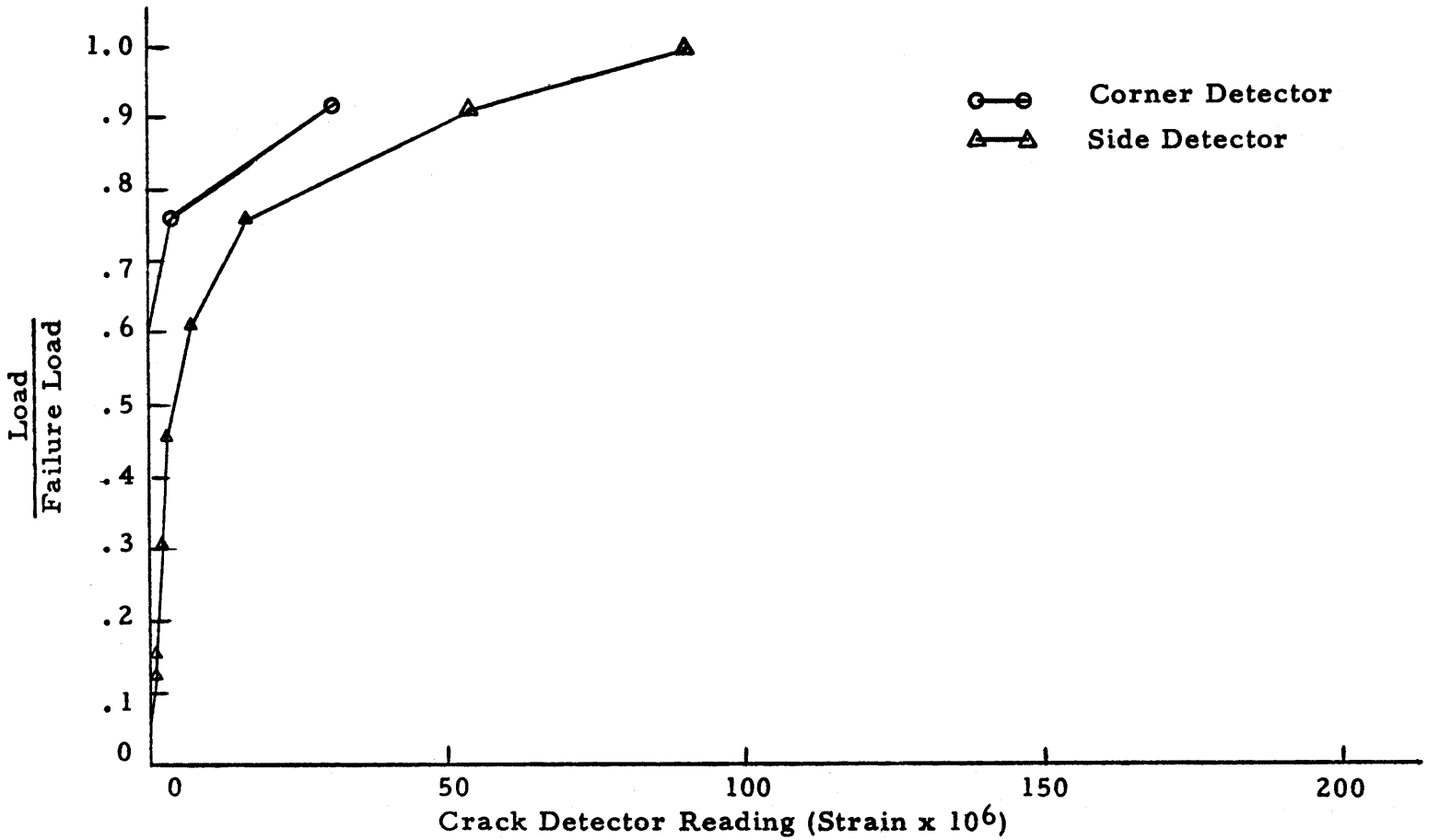


Fig. B. 3. Variation of Crack Detector Reading with Load/Failure Load for Slab 4S2 - 8

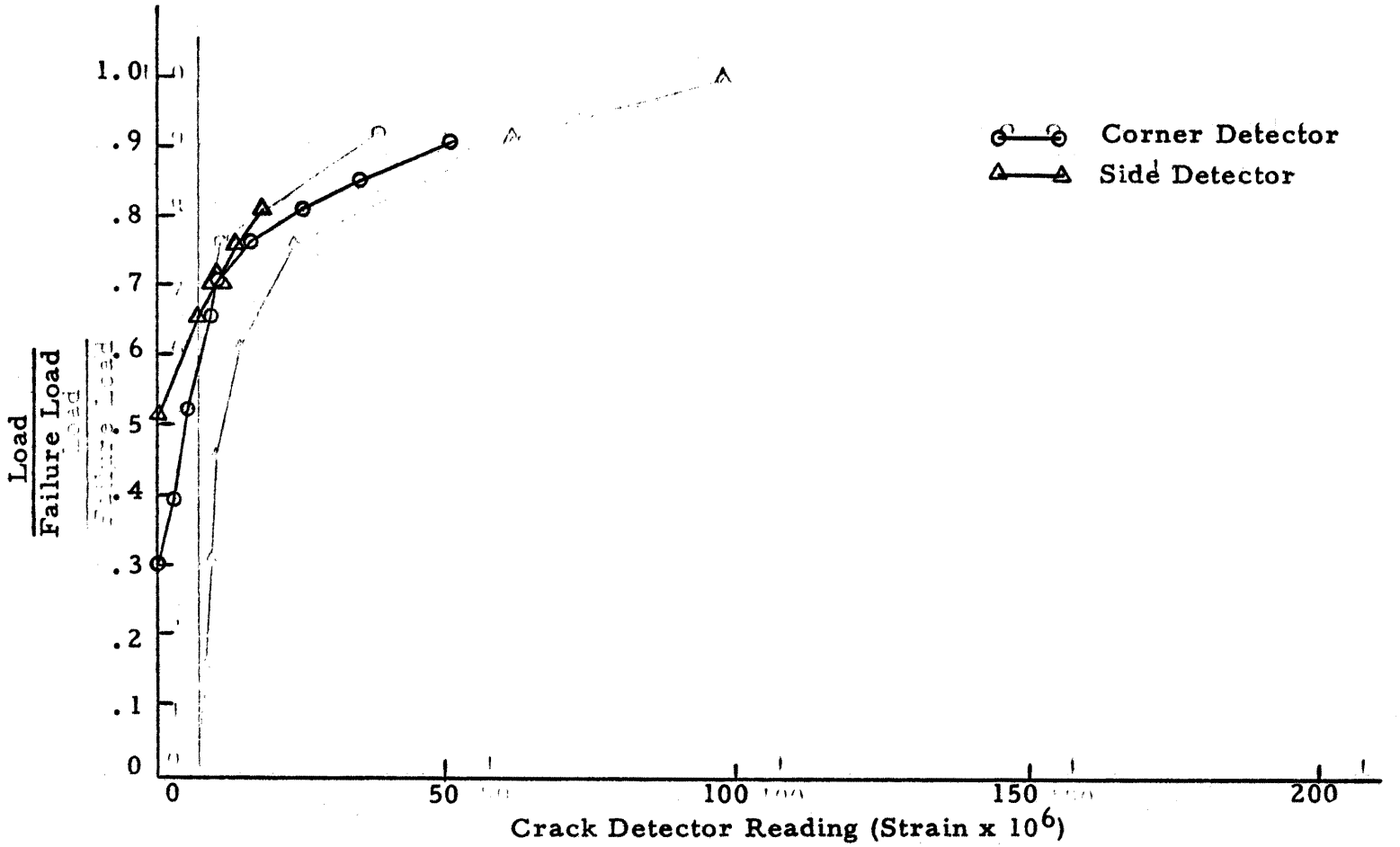


Fig. B.4. Variation in Crack Detector Reading with Load/Failure Load for Slab 4C1 - 12

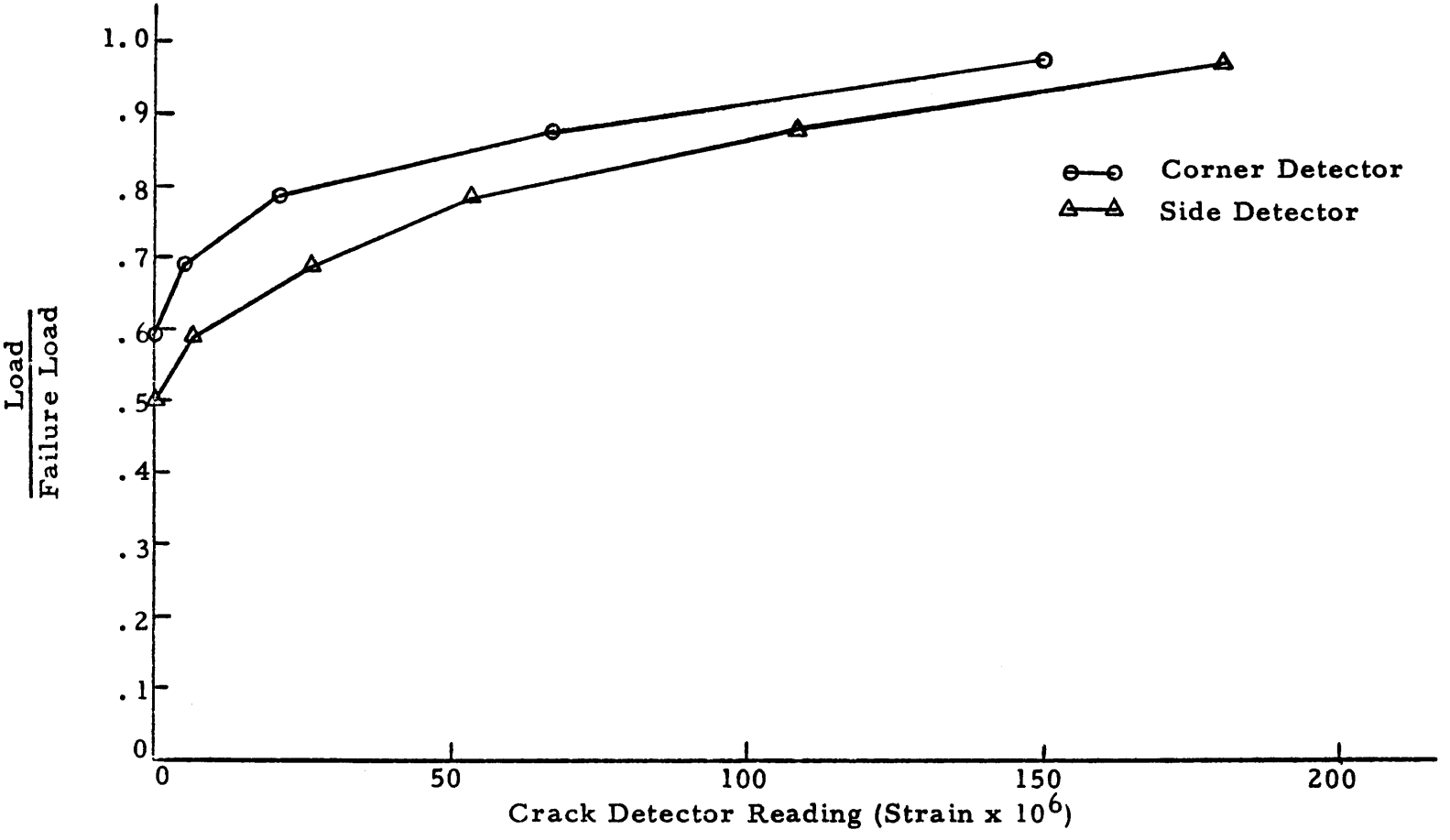


Fig. B.5. Variation in Crack Detector Reading with Load/Failure Load for Slab 8C1 - 13